## Universal cooling of quantum systems via randomized measurements

Josias Langbehn,<sup>1</sup> George Mouloudakis <sup>0</sup>,<sup>1</sup> Emma King <sup>0</sup>,<sup>2</sup> Raphaël Menu <sup>0</sup>,<sup>2</sup> Igor Gornyi <sup>0</sup>,<sup>3</sup> Giovanna Morigi <sup>0</sup>,<sup>2</sup> Yuval Gefen,<sup>4</sup> and Christiane P. Koch <sup>0</sup>,\*

<sup>1</sup>Freie Universität Berlin, Fachbereich Physik and Dahlem Center for Complex Quantum Systems, Arnimallee 14, 14195 Berlin

<sup>2</sup>Theoretical Physics, Department of Physics, Saarland University, 66123 Saarbrücken, Germany

<sup>3</sup>Institute for Quantum Materials and Technologies and Institut für Theorie der Kondensierten Materie,

Karlsruhe Institute of Technology, Karlsruhe 76131, Germany

<sup>4</sup>Department of Condensed Matter Physics, Weizmann Institute of Science, Rehovot 7610001, Israel

(Dated: July 28, 2025)

Designing cooling protocols is believed to require knowledge of the system spectrum. In contrast, cooling in nature occurs whenever the system is coupled to a cold bath. How does nature know how to cool? A natural cold bath can be mimicked with a reservoir of "meter" qubits that are initialized in their ground state. We show that a quantum system can be cooled without knowledge of system details when system-meter interactions and meter splittings are chosen randomly. For sufficiently small interaction strengths and long interaction times, the protocol ensures that resonant energy-exchange processes, leading to cooling, dominate over heating. Effectively, the dynamics is then captured by the rotating-wave approximation, which we identify as the basic mechanism for robust and scalable cooling of complex quantum systems through generic, structure-independent protocols. This offers a versatile universal framework for controlling quantum matter far from equilibrium, in particular, for quantum computing and simulation.

## I. INTRODUCTION

The development of efficient techniques to cool quantum systems has been instrumental for the emergence of quantum technologies. Laser cooling of atoms [1–3] paved the way for many identical quantum systems to be prepared in a pure quantum state. Extensions of laser cooling to the sideband and sympathetic cooling were pivotal to leveraging entanglement for a practical advantage in quantum logic spectroscopy [4]. The necessity to freeze out all the degrees of freedom that are not relevant to the encoding and processing of quantum information is even more imperative in solid-state platforms. Superconducting qubits, for example, are kept in dilution refrigerators to ensure quantum coherence [5].

In addition to maintaining sufficiently long lifetimes of quantum states, the operation of quantum hardware also requires the ability to prepare a set of qubits in a non-trivial fiducial pure state [6] and manipulate this state, avoiding unwanted excitations or decoherence. This represents a major factor limiting the speed and duration of coherent operations for most architectures. Clearly, present-day quantum platforms would benefit from the advancement of universal cooling strategies, since noise and crosstalk due to uncontrolled interactions between qubits severely limit the reachable circuit depths, as well as the fidelity of the engineered states [7, 8]. Further, cooling could be useful for quantum algorithms that rely on measuring the energy of the final state, such as variational quantum algorithms [9–11].

One difficulty in qubit reset and cooling in general is the export of entropy [12] — it requires an environment

into which entropy can be discarded. A possible approach to achieve this is by weakly coupling a "natural" bath, kept at low temperature, to the system. Other established techniques can render the entropy export more controllable and efficient. For example, the fastest way to reset a qubit is resonant energy exchange with an auxiliary qubit that is then discarded [13, 14], which is, however, based on knowledge about the system, here the relevant energy gap. Similarly, laser cooling relies on (near-) resonant excitation of optical transitions in a closed cycle [1–3], which becomes increasingly difficult for more complex systems and has hampered, e.g., the laser cooling of molecules [15]. In general, the cooling efficiency of a quantum system relies on the design of scattering processes that lead to energy extraction and overcome all other unwanted incoherent processes. This becomes challenging with increasing system complexity, where uncontrollable couplings with detrimental environments may be present or ergodicity may be broken due to symmetries. Take the example of cooling many-body quantum systems relevant to quantum simulations and quantum annealing. Not only are their spectra increasingly complex, but, by construction, generically unknown, making it difficult to devise suitable cooling schemes. Dissipative state preparation protocols [16–21] do require some knowledge of the system's spectrum, such as the spectral gap. Likewise, measurement-based steering of quantum states which drives the system towards a predesignated target state by quasi-local measurements [22–26] also requires knowledge of the system's degrees of freedom (and possibly Hamiltonian).

These examples underline the challenge of devising cooling protocols with practically no knowledge of the system at hand. Here we address this problem by leveraging an analogy with nature: Why can a generic quantum system be cooled by a low-temperature bath, irrespective

<sup>\*</sup> christiane.koch@fu-berlin.de

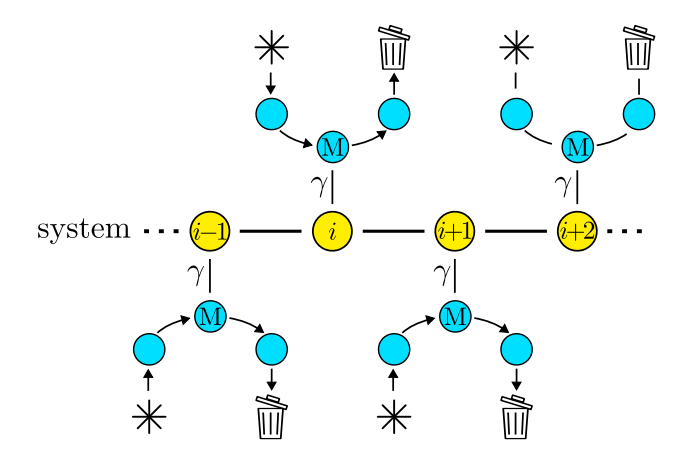


FIG. 1. Universal cooling via repeated, stochastically chosen interactions with meter qubits: Each constituent of the system is coupled to a meter qubit with coupling strength  $\gamma$ . The meter qubits are initialized in their ground states and interact sequentially with the system for time  $t_M$  after which they are discarded.

of its internal Hamiltonian? The strategy for mimicking a cold bath to cool, or, more precisely, to thermalize a many-body quantum system is illustrated in Fig. 1: The cold bath, acting as a sink for both entropy and energy, is represented by a set of auxiliary "meter" qubits that are initialized in their ground state. They are coupled locally with system degrees of freedom (depicted in yellow in Fig. 1) and, after a fixed interaction (or "measurement") time  $t_M$ , are discarded and replaced with identically initialized meters. The process is repeated until the steadystate energy is attained with a given fidelity [27]. This scheme has been turned into practical protocols in the context of measurement-induced dynamics [22–25, 28– 40], dissipative state preparation [16-21, 41-52], heatbath algorithm cooling [53–66], collision models [67–70], or quantum-feedback cooling [71–75]. Yet, the analogy with cooling in nature has not been fully explored; in particular, these protocols have not been designed to be system-agnostic. Attempts to reduce the required knowledge of the spectrum include sweeping the splitting of the meter qubits [61] and randomizing coupling operators [50] or interaction times [66]. These advances are important in view of practical implementations, but they do not answer the question how and why a system can be cooled without full knowledge of its spectral properties and symmetries.

Here, we establish stochasticity together with weak coupling as the general principle underlying universal cooling. We show that, in order to be as system-agnostic as possible, both the splittings of the meter qubits and the system-meter interactions have to be chosen randomly. Then, for small couplings  $\gamma$  and long interaction times  $t_M$ , the steady-state energy is proportional to  $\gamma$  and inversely proportional to  $t_M$ . In this regime, stochasticity ensures that resonant energy exchange, which leads to cooling, is favored over non-resonant processes that may

result in heating, akin to a rotating-wave approximation. Remarkably, two-body interactions—the simplest possible choice for the system-meter interaction—are sufficient for cooling. Despite the local coupling, the Kraus operators that we derive in the limit of weak coupling and long interaction times are effectively non-local, an expected key requirement for the cooling of a generic many-body quantum system [43, 50, 58]. Our protocol allows for cooling without the need to tailor the procedure to the system's details; rather, only an estimate of the system's spectral radius is required. The price for this agnosticity is the longer cooling time that is larger than those in approaches based on, e.g., feedback [24] or learning [65]. Moreover, the cooling times are determined not just by stochastic convergence but also by the minimal spectral gap, which sets the scale for weak coupling. At the same time, our protocol, on top of being closest to mimicking thermalization with a natural bath, is astonishingly simple to implement.

## II. RESULTS

The setup, combining the system of interest S and the meter qubits, evolves under the Hamiltonian

$$H_{\text{tot}} = H_{\text{S}} + H_{\text{SM}} + H_{\text{M}}, \qquad (1)$$

where  $H_{\rm S}$  and  $H_{\rm M}$  act on the system and meter qubits, respectively, and their coupling is given by  $H_{\rm SM}$ . If the spectrum of  $H_{\rm S}$  is known, the cooling process can be optimized by tailoring  $H_{\rm SM}$  and  $H_{\rm M}$  accordingly. Instead, our work is motivated by the observation that when a system is immersed in a cold bath, it thermalizes to the bath's temperature even though the bath is not specifically tailored to the system, i.e., the bath is system-agnostic. To obtain a cooling protocol without making assumptions about the system other than that it consists of quantum degrees of freedom with local couplings, we average over both the form of the system-meter interaction  $H_{\rm SM}$  and the level splitting of the meter qubits.

The cooling protocol is illustrated in Fig. 1 for the example of a one-dimensional many-body quantum system. It consists of repeating the following steps. First, the meter qubits are prepared in the ground state of their corresponding Hamiltonian  $H_{\rm M}=(\omega_{\rm M}/2)\,\tau_z$ , where  $\tau_z$  is the Pauli-z operator of the meter and the level splitting  $\omega_{\rm M}$  is chosen at random. In the second step, the meters and the system interact locally for an interaction time  $t_M$  where the form of the interaction  $H_{\rm SM}$  is also chosen randomly. Finally, after the interaction time, the system and the meter are decoupled, the meters are discarded, and the cycle is repeated starting from step 1 with a different random value of  $\omega_{\rm M}$  and a different form of the system-meter coupling.

## A. Asymptotic limit of random measurements

After many iterations of the protocol, the system will approach the steady state. We now show that it is related to the averaged completely positive trace-preserving (CPTP) map  $\vec{\mathcal{V}}$  for one iteration with randomized splittings and couplings: Initially, the system and all meter qubits are uncorrelated,  $\rho(0) = \rho_{\rm S}(0) \otimes |\vec{0}\rangle\langle\vec{0}|$  where  $|\vec{0}\rangle$  is the product state of the meter ground states. Describing the system-meter interactions by the unitary  $U(t) = \sum_{\vec{i},\vec{j}} U_{\vec{i},\vec{j}}(t) |\vec{i}\rangle\langle\vec{j}|$ , the global state at time t is  $\rho(t) = U(t)\rho_{\rm S}(0) \otimes |\vec{0}\rangle\langle\vec{0}|U^{\dagger}(t)$ . Tracing out the meters, the reduced state of the system after one iteration is given by

$$\rho_{\mathcal{S}}(t_M) = \sum_{\vec{i}} \langle \vec{i} | U(t_M) \rho_{\mathcal{S}}(0) \otimes | \vec{0} \rangle \langle \vec{0} | U^{\dagger}(t_M) | \vec{i} \rangle 
= \sum_{\vec{i}} U_{\vec{i}, \vec{0}}(t_M) \rho_{\mathcal{S}}(0) U_{\vec{i}, \vec{0}}^{\dagger}(t_M) = \mathcal{V} \rho_{\mathcal{S}}(0) , \quad (2)$$

where  $\mathcal{V}$  is a CPTP map describing the incoherent dynamics emerging from the interaction with the meters. To describe a stochastic average over many interactions, we parametrize the interaction  $H_{\rm SM}$  and choice of meter splitting in terms of a vector  $\vec{r}_n$ , such that the CPTP map at iteration n becomes  $\mathcal{V}(\vec{r}_n)$ . Averaging over all possible choices of system-meter interaction and meter splittings implies

$$\bar{\mathcal{V}} = \frac{1}{\mathcal{N}} \int d\vec{r} \, \mathcal{V}(\vec{r})$$

with fixed variance and suitable normalization  $\mathcal{N}$ . The averaged state of the system after n iterations is then obtained by integrating over all parameters  $\vec{r}_n$ :

$$\bar{\rho}_{S}(n t_{M}) \equiv \frac{1}{\mathcal{N}^{n}} \int d\vec{r}_{n} \dots d\vec{r}_{1} \mathcal{V}(\vec{r}_{n}) \dots \mathcal{V}(\vec{r}_{1}) \rho_{S}(0)$$
$$= \bar{\mathcal{V}}^{n} \rho_{S}(0) . \tag{3}$$

Note that  $\bar{\rho}_{\rm S}(n\,t_M)$  is the mean value of the distribution of state trajectories after n repetitions. An individual trajectory is denoted as  $\rho_S\left(\vec{r}_n,\ldots,\vec{r}_1\right)=\mathcal{V}(\vec{r}_n)\ldots\mathcal{V}(\vec{r}_1)\rho_S(0)$  and we expect that  $\rho_S(\vec{r}_n,\ldots,\vec{r}_1)\to\bar{\rho}_S(n\,t_M)$  as  $n\to\infty$ , i.e., the variance of the distribution of states vanishes only as  $n\to\infty$ . Nevertheless, all steady-state properties can be extracted from  $\bar{\mathcal{V}}$  by calculating its fixed point. In other words, the system state at the asymptotic time  $t=nt_M$  can be deduced, as  $n\to\infty$ , from the CPTP map for a single iteration, averaged over all system-meter interactions.

To first order in system-meter coupling strength, our protocol is equivalent to coupling the system to a bath composed of all possible meter realizations [69, 70], as we also show in appendix A. Next, we will use the example of a two-level system to identify the conditions on the system-meter coupling strength  $\gamma$  and interaction time  $t_M$  that ensure cooling towards the ground state of  $H_S$ .

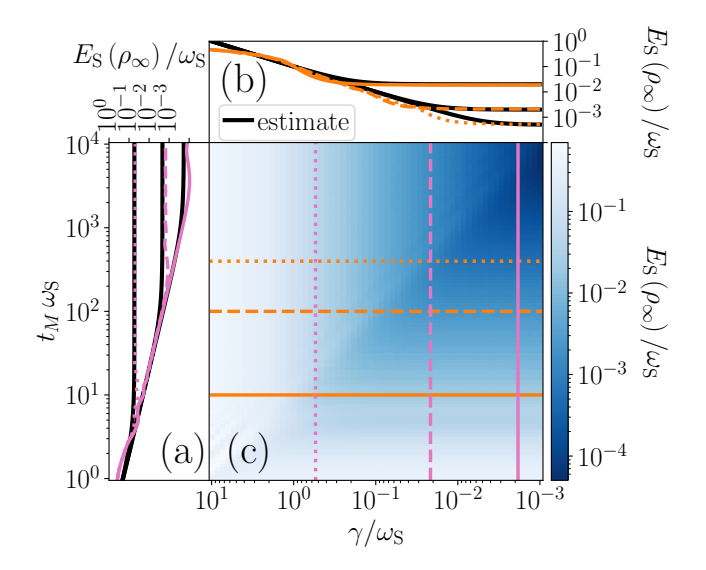


FIG. 2. Cooling a two-level system: Steady-state energy  $E_{\rm S}(\rho_{\infty})$  as a function of system-meter coupling strength  $\gamma$  and interaction time  $t_M$  with cuts along  $t_M$  and  $\gamma$  presented, respectively, in (a) and (b) by the corresponding (dotted, dashed, and solid) magenta and orange curves. The steady-state energy follows the estimate (7) for  $\omega_{\rm S}\gg 1/t_M$  and  $\omega_{\rm S}\gg \gamma$ , as indicated by the black curves.

#### B. Cooling a qubit

To consider the cooling of a single qubit, we write its Hamiltonian as

$$H_{\rm S} = \frac{\omega_{\rm S}}{2} \, \vec{v} \cdot \vec{\sigma} \,, \tag{4}$$

where  $\omega_{\rm S}$  is the system qubit's level splitting,  $\vec{v}$  the quantization axis in the Bloch sphere, and  $\vec{\sigma}$  the vector of Pauli matrices. We choose

$$H_{\rm SM} = \gamma \, \sigma(\theta, \phi) \otimes \tau_x, \tag{5}$$

where  $\sigma(\theta, \phi)$  is a Pauli matrix representing quantization along the direction corresponding to angles  $\theta$  and  $\phi$  on the Bloch sphere. The Hamiltonian of the meter qubits is

$$H_{\rm M} = \frac{\omega_{\rm M}}{2} \, \tau_z,\tag{6}$$

where  $\omega_{\rm M}$  is the level splitting of the meter (given in the laboratory frame). We choose, without loss of generality,  $\omega_{\rm M}>0$ , such that the meter's ground state is  $|\downarrow\rangle$ . The interaction between the system qubit and the meter leads to a CPTP map  $\mathcal{V}(\theta,\phi,\omega_{\rm M})$  that describes the evolution of the system from iteration n to n+1. The steady state is obtained by averaging  $\mathcal{V}(\theta,\phi,\omega_{\rm M})$  over the Bloch sphere and uniformly over  $\omega_{\rm M}\in[0.1|\omega_{\rm S}|,3|\omega_{\rm S}|]$ . This choice of  $\omega_{\rm M}$  only requires knowledge of the spectral radius of  $H_{\rm S}$ , such as to cover all possible transitions. Initializing the meter in its ground state ensures that the meter can absorb energy and mirrors a bath at low temperature.

Figure 2 shows the system energy in steady state  $\rho_{\infty}$  as a function of the coupling strength  $\gamma$  and the interaction time  $t_M$ . A significant reduction of the qubit's energy compared to the initial value is observed, which indicates that the system is efficiently cooled down by randomized interactions with the meter. For large  $t_M$  and small  $\gamma$ , the system energy deviates from the ground-state energy by approximately  $10^{-3}\omega_{\rm S}$ , which we refer to as the error. Notably, in Fig. 2a, the steady-state energy decreases as  $1/t_M$  as long as  $\omega_S \gg 1/t_M \gg \gamma$ . When  $1/t_M$  becomes comparable to  $\gamma$ , the energy as a function of  $1/t_M$  reaches a saturation limit, cf. the different onsets of the saturation regimes for the three different values of  $\gamma$ . Similarly, Fig. 2b shows a decrease of the steady-state energy as a function of  $\gamma$  as long as  $\gamma \gg 1/t_M$ . Once  $\gamma$  becomes comparable to  $1/t_M$ , the energy as a function of  $\gamma$  saturates, as illustrated by the onset of the saturation regime for three values of  $1/t_M$ .

The dependence of the steady-state energy on  $\gamma$  and  $1/t_M$  observed in Figs. 2a and 2b implies that cooling the system towards its ground state is possible with an arbitrarily low error by increasing  $t_M$  and reducing  $\gamma$  at the same time. Indeed, generically, for  $\omega_{\rm S} t_M \to \infty$  and  $\gamma/\omega_{\rm S} \to 0$ , the system's steady state tends to the ground state (see appendix B). For the regime of weak coupling and long interaction times,  $\omega_{\rm S} \gg 1/t_M$ ,  $\gamma$ , we estimate the steady-state energy as

$$E_{\rm S} \approx E_{\rm est} \equiv \sqrt{(\gamma/2)^2 + 1/t_M^2},$$
 (7)

and find qualitative agreement with numerical simulation, as indicated by the black curves in Figs. 2a and 2b.

### C. Why cooling works

We now show that weak coupling and long interaction times ensure an effective implementation of resonant energy exchange between the system and meters and, thus, universal cooling. It is akin to effectively implementing a rotating-wave approximation (RWA). To see this, assume for a moment that the system's quantization axis is along z,

$$H_{\rm S} = \frac{\omega_{\rm S}}{2} \, \sigma_z \,, \tag{8}$$

and the system-meter coupling is given by

$$H_{\rm SM} = \gamma \, \sigma_x \otimes \tau_x \,. \tag{9}$$

This coupling comprises both co-rotating and counterrotating terms,

$$H_{\rm SM} = \underbrace{\frac{\gamma}{2} (\sigma_{+} \tau_{-} + \sigma_{-} \tau_{+})}_{H_{+-}} + \underbrace{\frac{\gamma}{2} (\sigma_{+} \tau_{+} + \sigma_{-} \tau_{-})}_{H_{++}}. \tag{10}$$

where  $\sigma_{+} = |\uparrow\rangle\langle\downarrow|$ ,  $\sigma_{-} = \sigma_{+}^{\dagger}$ , and equivalently for the meter operators  $\tau_{\pm}$ . For  $\omega_{\rm S} > 0$  in Eq. (8), the counterrotating term is  $H_{++}$  and the co-rotating term is  $H_{+-}$ , but their roles are swapped for the opposite sign of  $\omega_{\rm S}$ . Under the RWA, one neglects the counter-rotating term and retains only the co-rotating one.

The co-rotating interaction necessarily increases the meter's energy by transferring energy from the system (or keeps it constant in the rare case of the interaction time matching a full return of the excitation) since the meter is initialized in its ground state. Repeated meter resets then lead to cooling of the system. Indeed, it is well-known that a (partial) swap generated by the co-rotating terms is the unique unitary that leads to thermalization irrespective of initial system and meter states [67, 76]. In contrast, the counter-rotating interaction describes the simultaneous excitation (or de-excitation) of both the system and the meter. This can lead to an increase in the energy of both parties due to the accumulation of negative energy in the interaction term  $H_{\rm SM}$ .

Incidentally, the single-qubit steering protocol of Ref. [22] realizes the counter-rotating interaction with  $H_{\rm SM}=H_{+-}$ , assuming  $\omega_{\rm S}<0$  (while the co-rotating term is absent). Then the target state of the system qubit is identical to the initial state of the meter. While  $|\downarrow\rangle$  is the ground state for the meter, it is the excited state for the system with  $\omega_{\rm S}<0$ . As a result, the steering protocol leads to heating rather than cooling of the system qubit; see details in appendix C, as well as Ref. [64].

This example is important as it contradicts the naive expectation that fresh meters always form a zero-temperature bath that cools the system. It also elucidates the crucial role of resonant energy exchange for cooling when both co- and counter-rotating terms are present in the system-meter coupling. Indeed, within the RWA, the detrimental process of the "counter-rotating heating" is suppressed to first order in  $\gamma$ . We thus conjecture that our protocol is based on effectively realizing system-meter interactions in the RWA. The RWA is valid under the following conditions (see also appendix D):

$$\begin{split} \frac{||\omega_{\rm S}| - \omega_{\rm M}|}{|\omega_{\rm S}| + \omega_{\rm M}} \ll 1 & \text{(near resonance), (11a)} \\ \gamma \ll |\omega_{\rm S}| + \omega_{\rm M} & \text{(weak coupling), (11b)} \\ 1/\left(|\omega_{\rm S}| + \omega_{\rm M}\right) \ll t_{M} & \text{(long interaction time). (11c)} \end{split}$$

With the energy gap  $\omega_{\rm S}$  unknown and  $\omega_{\rm M}$  chosen randomly, the resonance condition (11a) will only be fulfilled sometimes. This suggests that the requirements of weak coupling (11b) and long interaction times (11c), already identified in our discussion of Fig. 2 above, are sufficient to effectively ensure the RWA. We analyze this in detail below.

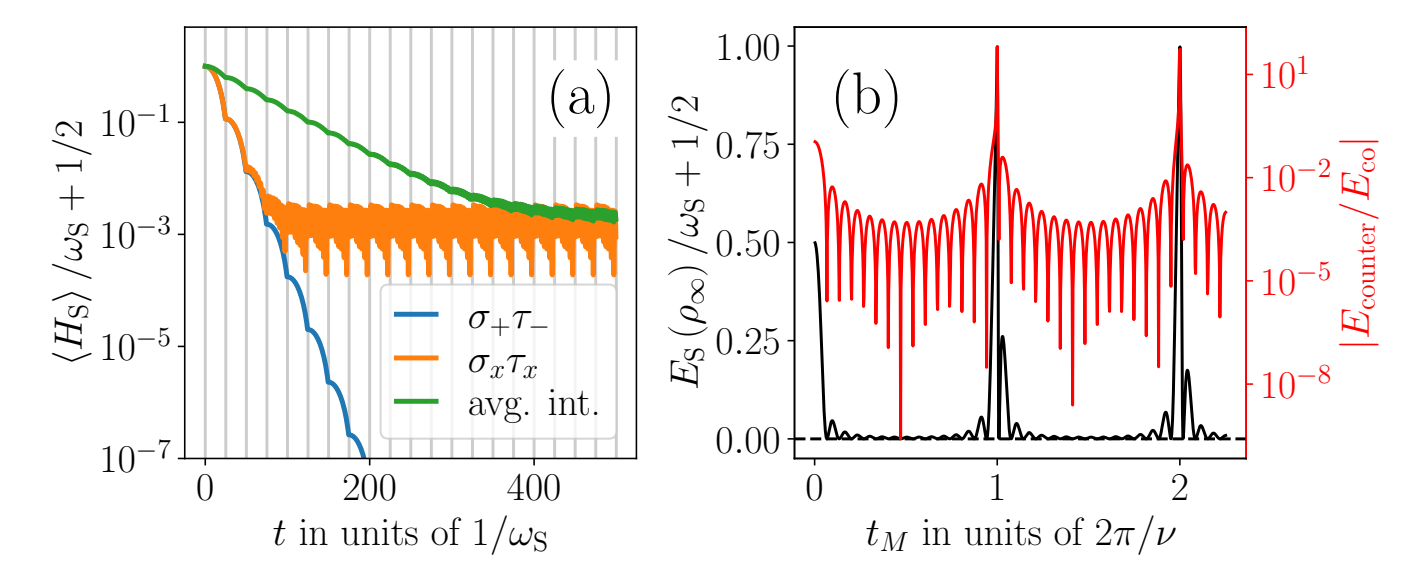


FIG. 3. Dynamics of cooling a two-level system via repeated interactions: (a) System energy as a function of time for three different types of system-meter interaction corresponding to different levels of knowledge about the system. Stochastically averaged interactions (green) are used in the case of no knowledge, whereas  $\sigma_x \tau_x$  (orange) and  $\sigma_+ \tau_-$  (blue) couplings imply, respectively, knowledge of the quantization axis and knowledge of both the quantization axis and the gap sign. Note that in general the system attains a stroboscopic steady state, i.e, at  $t = nt_M$  when the meter is reset (indicated by faint vertical lines). In between measurements, the system energy can still show oscillations. (b) Steady-state energy (black) and the ratio of contributions to the steady-state energy associated with the counter- and co-rotating interactions (red), displaying revivals of the co-rotating terms at integer multiples of  $\nu t_M/2\pi$ , where  $\nu$  is an eigenfrequency of  $H_{\rm tot}$ , Eq. (12). Except for the close vicinity of these values, the RWA is valid since the co-rotating contributions to the system energy dominate over the counter-rotating ones. Hence, except for singular unfortunate choices of  $t_M$ , the system energy can be reduced, implying efficient cooling. Parameters for both panels are  $\omega_S > 0$ ,  $\gamma = 0.1\omega_S$ , and  $\omega_M = \omega_S$ .

## D. Role of co-rotating and counter-rotating terms in cooling a qubit

Figure 3a presents the time evolution of the system energy under repeated meter resets for different choices of  $H_{\rm SM}$ , corresponding to different levels of knowledge about the system. Assuming full knowledge of the system (quantization axis as well as the sign of  $\omega_{\rm S}$ , taken here  $\omega_S > 0$ ), one can engineer the system-meter interaction such that it coincides with the co-rotating term  $H_{+-}$  (represented by the blue curve in Fig. 3a). Not surprisingly, the result is very efficient cooling toward the ground state. Next, assume that the system's quantization axis is known, while the sign of  $\omega_{\rm S}$  is not. A detailed analytical derivation for this case is presented in appendix C. As discussed above, for  $\omega_{\rm S}$  < 0, the interaction  $H_{+-}$  would lead to heating of the system because the roles of co- and counter-rotating interactions are reversed. Therefore, to be able to cool the system for both  $\omega_{\rm S} > 0$  and  $\omega_{\rm S} < 0$ , both  $H_{+-}$  and  $H_{++}$  must be present; in other words, the interaction must be of the form  $\sigma_x \tau_x$ (orange curve in Fig. 3a). The important feature here is that  $\sigma_x$  is perpendicular to  $\sigma_z$ , i.e.,  $\sigma_x$  acting on one of the  $\sigma_z$ -eigenstates maps it to the other one. In contrast to perfect cooling (blue curve), the orange curve does not approach the ground-state energy, but the residual system energy is much lower than the initial one, and this

error can be made smaller by choice of  $\gamma$  and  $t_M$ , according to Fig. 2 and in line with Eqs. (11b, 11c). Finally, if the quantization axis is also unknown, the best one can do is to choose the direction of the interaction randomly (green curve in Fig. 3a). Then the co-rotating part of the interaction (with respect to the unknown system's quantization axis) is dominant at some steps of the protocol, which, on average, overcomes the unwanted heating at other steps. While the cooling rate for the green curve is lower than that for the protocols tailored to the system, the final energy eventually approaches the value attained for a known quantization axis (orange curve in Fig. 3a). Again, the residual system energy depends on the systemmeter coupling strength and interaction time, cf. Fig. 2, and can be made arbitrarily small. This demonstrates that randomization of the system-meter coupling can efficiently cool a single qubit without knowing the sign of the gap and the quantization axis. Note that in the case of  $\sigma_x \tau_x$  or averaged coupling (orange and green curves), the system energy in Fig. 3a shows oscillatory behavior between measurements. That is to say, the system converges stroboscopically to the steady state at times  $t = nt_{\rm M}$  when the meter is reset. This poses no practical limitation because eventually we are interested in the system at long times, after it is decoupled from the meter.

Taking the interaction to be of the form  $\sigma_x \tau_x$ , the rela-

tion between cooling and the role of the co- and counterrotating terms for  $\omega_{\rm S}>0$  is illustrated in Fig. 3b. It compares the energy of the system's steady state as a function of interaction time  $t_M$  (black curve, left y-axis labels) to the ratio  $E_{\rm counter}/E_{\rm co}$  of the system energies associated with the counter-rotating and co-rotating interactions (red, right y-axis labels). The smaller the ratio, i.e., the more the "co-rotating interaction energy" dominates over its counter-rotating counterpart, the lower is the steady-state energy. In other words, the better the RWA is obeyed, the colder the system becomes.

Figure 3b also shows that the steady-state energy depends on the choice of the interaction time  $t_M$ . In particular, for integer multiples of  $\nu t_M/2\pi$ , where  $\nu$  is one of the eigenfrequencies of  $H_{\rm tot}$  [Eq. (1); see appendix C],

$$\nu = \sqrt{\gamma^2 + (\omega_{\rm S} - \omega_{\rm M})^2}, \qquad (12)$$

"revivals" of the counter-rotating contributions to the energy are observed. At these interaction times, the energy associated with the co-rotating processes is swapped from the system to the meter and back, such that  $E_{\rm co}$  becomes small in comparison to the counter-rotating contribution  $E_{\rm counter}$ . This may lead to heating of the system. In practice, this does not pose a significant obstacle, since the effect occurs only for relatively isolated values of  $t_M$ . Moreover, the position of the revivals depends on the specific interaction and meter splitting. Since we investigate stochastic choices of those parameters, we expect that, on average, these peaks are suppressed (the same would also happen for randomized values of  $t_M$  [66]).

#### E. Cooling a many-body system

We now show that many-body systems can be cooled employing the same technique of randomized repeated interactions with the meter qubits. This generalization from the single-qubit case is possible despite several additional difficulties that arise for cooling many-body systems:

- 1. Multiple transition frequencies: Unlike a qubit, where there is a single transition frequency between the ground and excited states, many-body systems have multiple levels and transition frequencies that need to be addressed by the measurement qubits.
- 2. Symmetry-protected subspaces: For many-body systems, there may be symmetry-protected subspaces in the system's Hilbert space. When  $H_{\rm S}$  is unknown, the symmetries it supports are also unknown, making it difficult to break the symmetries in order to make protected subspaces accessible to cooling.
- 3. Frustration: Frustrated many-body systems cannot be steered to the ground state by (quasi-)local system-meter couplings [77, 78]. In this case, trying to cool the system by respecting individually

the competing local terms in  $H_{\rm S}$  (i.e., by attempting to reduce the energy with respect to the quasilocal terms in the Hamiltonian) will not allow for cooling all the way to the ground state energy.

In order to discuss a class of systems that feature all of the above, we consider a Heisenberg chain of size N with the Hamiltonian

$$H_{\rm S} = \sum_{i=1}^{N} J_i \vec{S}_i \cdot \vec{S}_{i+1} \,, \tag{13}$$

where  $J_i < 0$   $(J_i > 0)$  corresponds to (anti-) ferromagnetic coupling between sites (i, i+1). Conserved quantities are the total spin operators  $\Sigma_{x,y,z} = \sum_i^N \sigma_{x,y,z,i}/2$  and  $\Sigma^2 = \Sigma_x^2 + \Sigma_y^2 + \Sigma_z^2$ . In our cooling protocol, each system spin is coupled with a meter qubit:

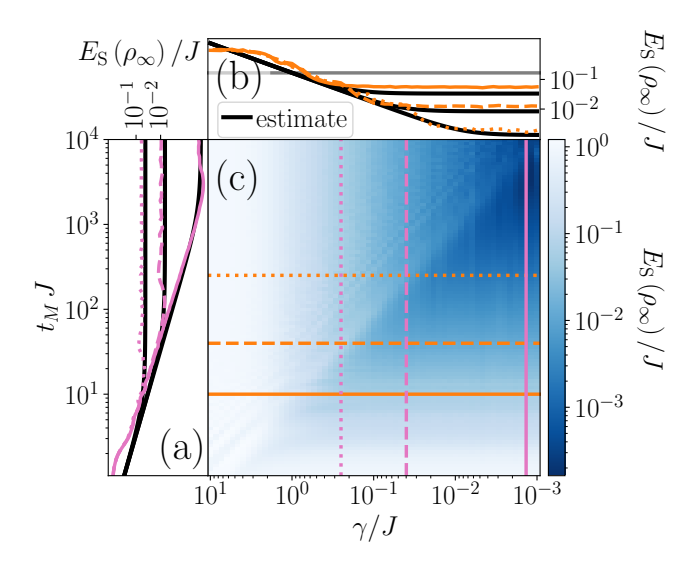
$$H_{\rm M} = \frac{\omega_{\rm M}}{2} \sum_{i} \tau_{z,i} \,, \tag{14}$$

$$H_{\rm SM} = \frac{\gamma}{2} \sum_{i} A_i(\theta, \phi) \tau_{x,i} \,. \tag{15}$$

For simplicity, in a single iteration of the protocol, all meter qubits have the same level splitting  $\omega_{\rm M}$ , and all system spins are coupled to their corresponding meter qubits with the same coupling operator  $A_i$ . The steady-state energy of the system is calculated from the CPTP map  $\bar{\mathcal{V}}$ , averaged over the interactions  $A_i(\theta,\phi)$  on the Bloch sphere, and meter splittings are sampled uniformly from the interval  $\omega_{\rm M} \in [0,1.1\,\|H_{\rm S}\|]$ , requiring only knowledge of  $\|H_{\rm S}\|$ .

Figure 4a-4c displays the steady-state energy of the system for N=3 and J=(1,1,0). This is an antiferromagnetic Heisenberg chain with open boundary conditions; it is expected to show frustration making cooling potentially harder. The steady-state energy behaves qualitatively similarly to that in the single-qubit system, cf. Fig. 2. In particular, it approaches the groundstate energy within an error of about  $10^{-3}J$  for large  $t_M$  and small  $\gamma$  and follows the estimate (7) for weak coupling and long interaction times. This is in line with our interpretation of an effective RWA where resonant co-rotating interactions leading to cooling dominate over all other processes. Apparently, cooling by repeated randomized measurements can overcome the complications that emerge in many-body systems, which we identified above. We rationalize this as follows:

1. Regarding the multitude of transition frequencies, sampling  $\omega_{\rm M}$  from the interval  $[0,1.1\,||H_{\rm S}||]$  ensures that eventually a value is drawn, which is "sufficiently resonant" to any given transition in the system. Off-resonant values of  $\omega_{\rm M}$  are not detrimental, as the effective coupling between the system and meters is small in such cases. Crucially, even if the "wrong" values of  $\omega_{\rm M}$  (potentially leading to heating) are chosen more frequently, for weak coupling between system and meters, the heating



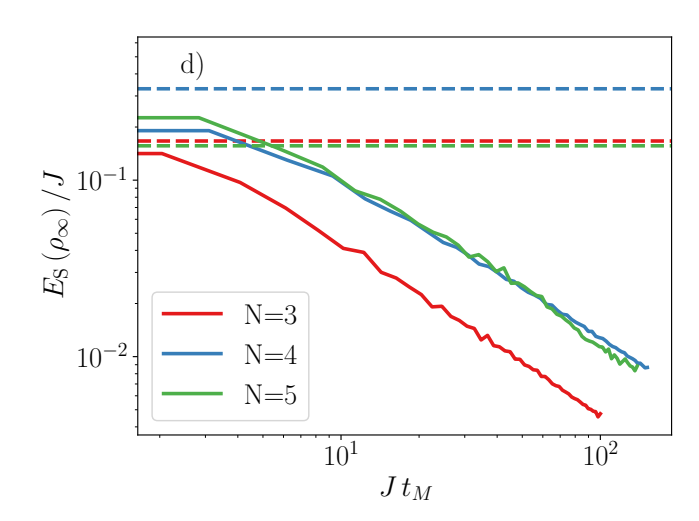


FIG. 4. Cooling a Heisenberg chain: (a-c) Steady-state energy as a function of system-meter interaction strength  $\gamma$  and interaction time  $t_M$  for N=3. As in the case of a two-level system (cf. Fig. 2), cooling works best for weak interactions and long interaction times, where it follows the estimate (7). (d) Steady-state energy of the system as a function of interaction time  $t_M$  for chain sizes N=3,4,5, all showing a scaling of the steady-state energy with  $1/t_M$ . The dashed lines indicate the lower bound on the energy obtainable by steering. Parameters are  $\omega_M \in [0, 1.1 ||H_S||]$  and  $\gamma = 10^{-3} J$  in (d).

rate is slower than the cooling rate that occurs for "good" values of  $\omega_{\rm M}$ . This is because sufficiently weak coupling and long interaction time realize the RWA (as illustrated in Fig. 3b for the two-level system), and after many repetitions, one can effectively cool down the system. Here, it is important to keep in mind that the meters, prior to interaction, are prepared in their ground state.

- 2. The issue of symmetries and symmetry-protected subspaces is resolved by randomizing the type of system-meter interactions. Here, resonant coupling to a meter qubit can be seen as a quasi-local perturbation that breaks the symmetry, and sampling the type of interaction randomly ensures that this will happen eventually, thus opening the protected subspace to cooling. At the same time, for interactions that do not break the symmetry, cooling within the protected subspaces is still possible. That being said, breaking symmetries with randomly chosen interactions may be slow, and the presence of symmetries will likely reduce the cooling speed.
- 3. Cooling systems with frustrated Hamiltonians ("unsteerable systems") requires a non-local action on the system. In our protocol, it is generated by the interplay of the system Hamiltonian and coupling to the meters when generating the time evolution. Even though the couplings within the Hamiltonian and between the system spins and meters are local (two-body in our example), the combined influence of local Hamiltonian evolution and repeated local resets leads, for sufficiently long interaction times  $t_M$ , to effectively non-local dynam-

ics. In other words, the propagation of excitations governed by  $H_{\rm S}$  effectively dresses the local Kraus operators introduced by  $H_{\rm SM}$ . The overall protocol thus realizes a non-local action on the system, which may overcome frustration, similarly to the circuit implementations of dissipative state preparation [50, 58].

The scaling of the steady-state energy with  $t_M$  is shown for system sizes N=3,4, and 5 in Fig. 4d, revealing the energy to be proportional to  $1/t_M$ , as also expected from the estimate (7). This scaling is compared with the lower bounds on the energy that can be obtained by means of steering [78], indicated by dashed lines. Cooling by repeated randomized system-meter interactions clearly outperforms steering for sufficiently large  $t_M$  and weak  $\gamma$  in view of the scaling of the steady-state energy with  $\gamma$  and  $1/t_M$ . This is discussed in more detail below.

## F. Comparison with steering

We compare cooling via repeated randomized systemmeter interactions to measurement-induced steering, which prepares desired quantum states using specifically engineered quasi-local system-meter interactions [22]. Passive or "blind" steering, discarding measurement readouts, works perfectly for non-frustrated systems, where the target state is the ground state of a parent Hamiltonian (for which all its local terms individually annihilate its ground state), even in the absence of the system Hamiltonian. In the presence of the system Hamiltonian, the same steering protocol amounts to cooling the system to its ground-state energy. Provided the system

is steerable, the ground state is reached with an error that decays exponentially in time. When the meter reset rate is sent to infinity (corresponding to the continuous limit of steering), the dynamics of the steered system is described by a Lindblad master equation,

$$\frac{d}{dt}\rho = -i[H_{\rm S}, \rho] + \kappa \sum_{i} \left( L_i \rho L_i^{\dagger} - \frac{1}{2} \{ L_i^{\dagger} L_i, \rho \} \right) . \quad (16)$$

Here, the quasi-local jump operators  $L_i$  are determined by the system-meter Hamiltonian [22, 48], and  $\kappa$  is the steering rate given in terms of the coupling strength to the meters.

Crucially, for frustrated systems, the lowest energy obtainable by steering is limited by the glass floor [78]. The term derives from an analogy to glassy systems featuring a rugged energy landscape, which are hard to cool. The underlying reason is frustration. Steering typically cannot go beyond a certain lowest energy, the glass floor, because it effectively aims at minimizing energies associated with the quasi-local terms that make up the Hamiltonian  $H_{\rm S}$ . But in frustrated systems, these terms do not have the global ground state as a common eigenstate with minimal energy. The value of the glass floor depends on the specific choice of the jump operators  $L_i$ . A lower bound on the glass floor can be obtained through a surrogate state construction [78], correspondingly referred to as surrogate bound. In Fig. 4d, the surrogate bound for the Heisenberg antiferromagnet is shown by the dashed lines. The figure demonstrates that cooling can undercut the surrogate bound and, therefore, randomized cooling wins over any attempt at cooling by steering for sufficiently large  $t_M$  and weak  $\gamma$ .

Finally, the system-meter interactions required to obtain the jump operators  $L_i$  for steering are typically non-trivial to engineer. For systems with nearest-neighbor interactions, for instance, one needs to engineer three-body interactions between two system sites and the meter qubit [48]. This complication is absent in the proposed cooling procedure, where two-body interactions that do not require any fine-tuning are sufficient. Thus, our nature-inspired approach for cooling quantum matter provides a versatile framework that, in general, is more efficient than steering-based cooling, both from an abstract and a practical perspective.

#### G. Limitations

The central result of this work is that universal cooling leads to a steady-state energy that can be arbitrarily reduced for large  $t_M$  and small  $\gamma$  according to Eq. (7). This estimate holds for weak coupling and long interaction times compared to the system's intrinsic energy scale. That is, a system can be cooled down as long as  $\Delta/\gamma \ll 1$  and  $\Delta t_M \gg 1$ , where  $\Delta$  is a typical transition energy in the system. This coincides with the regime of validity of the RWA, Eqs. (11b)-(11c), supporting the

idea that the resonant processes captured by the RWA provide the key mechanism allowing cooling to be universal.

In many-body systems, energy gaps  $\Delta$  can be very small, especially close to the ground state. At first glance, this appears to be a potential obstacle for cooling: For  $\Delta$  comparable to  $\gamma$ , the coupling to the meter may not be able to resolve the ground and first excited many-body levels. One would thus expect fluctuations between these two levels. In practice, the system will thermalize to the temperature of the meter ensemble. For a single-qubit system, we have investigated the implications of a meter prepared in a thermal state with finite temperature in appendix C. We have found that the occupation number of the meter gets transferred to the system's steady state. This confirms that the effective temperature found in the system's steady state is limited by the temperature of the meter, as one would expect.

### III. DISCUSSION AND OUTLOOK

Here we have shown that combining the wellestablished technique of repeatedly resetting auxiliary degrees of freedom [41] with stochastic system-meter interactions results in a system-agnostic cooling protocol. It is universal in the sense that lowering the energy is guaranteed as long as the coupling is weak and the inverse interaction time is small compared to the minimal energy gap. For many-body systems with non-degenerate ground states, preparation of the ground state is possible. Stochastic system-meter interactions imply that both heating and cooling processes will be realized in the various steps of the protocol. We have found that weak and long system-meter interactions ensure that "good" cooling interactions are much more efficient in extracting energy from the system than "bad" heating interactions in pumping energy into the system. The reason is that the heating processes are driven by the counter-rotating interactions, and weak and long system-meter interactions make sure these are negligible. An effective implementation of the rotating-wave approximation as the basis for universal cooling is the key insight that our work provides.

The simplicity of our approach sets it apart from steering protocols [22, 24, 50] which require one to engineer non-trivial system-meter interactions. Moreover, while steering efficiently prepares certain predesignated target states, paradoxically, it may give rise to heating when applied to a system whose microscopic parameters are not fully known [64]. When comparing our stochastic universal cooling to approaches that implement dissipative state preparation via circuit decompositions [19, 20, 50, 61], these protocols are expected to be faster and to thus require less resources in the form of meter qubits, while relying on similar or somewhat higher levels of knowledge about the system. Generally, a higher level of system knowledge correlates with better scaling

of the protocol. For example, the LogSweep algorithm for the transverse-field Ising model of Ref. [61] utilizes meter energy sweeps over a range that covers all possible system transitions to achieve cooling in polynomial times, but this assumes at least an estimate of the energy gap. On the other hand, the bang-bang-type protocols utilizing short, strong interactions to achieve rapid and depth-efficient cooling that have also been discussed [61], are susceptible to control errors and suffer from convergence issues as the cooling process may plateau at some residual excitation levels. Similarly, the logarithmic nature of the LogSweep algorithm [61] as well as dissipative state preparation using a spectral filter function [50] may be problematic when approaching sub-gap states. Moreover, the ingenuity of these sophisticated protocols requires some degree of control to be exerted, in contrast to our approach, where randomness of all parameters involving the meters is expected to make the procedure robust—indeed, any potential error in the implementation can be viewed as a source for randomness.

Our study opens the door to a host of challenging questions. An important issue is the scalability of our method. This concerns both the cooling time and its dependence on the system-meter coupling strength and interaction time, as the system size is increased, as well as the required number of meter qubits. Evidently, one should consider the possibility of a dilute-cooling variant of our protocol, analogously to dilute cooling with steering [48]. In terms of improving the cooling time, it could be advantageous to exploit the fact that sometimes a lowtemperature thermal state can be reached faster than a high-temperature one [79]. Moreover, active-decision protocols, which use the readout sequences to design the further protocol steps, may accelerate the preparation of target states [24–26, 80]. Similarly, our stochastic cooling protocol is likely to benefit from leveraging knowledge acquired from the measurement outcomes [65], e.g., by adapting the distribution from which the meter splittings and interactions are drawn, or from active decisionmaking based on the record of outcomes of the meters' projections. It will also be interesting to understand the performance of our method as a function of the energy landscape being more or less "glassy". Will the system get trapped in a metastable energy minimum, blocking its access to the true minimum, or is stochasticity sufficient to overcome such scenarios? In this respect, it is important to note the difference between cooling towards the ground state energy and attaining significant overlap with the ground state (high fidelity). This issue is particularly pertinent when the ground state is degenerate. Finally, one may consider combining our cooling approach with quantum annealing, where the system Hamiltonian is slowly varied in time. It is an example where cooling of undesired excitations can only work if it is fully system-agnostic. Universal cooling has the potential to significantly improve the efficacy of quantum annealing.

#### ACKNOWLEDGMENTS

We acknowledge helpful discussions with Yi-Xuan Wang, Kyrylo Snizhko, Yaroslav Herasymenko, Lin Lin, and Shovan Dutta. Financial support from the Deutsche Forschungsgemeinschaft (DFG) through the Collaborative Research Centre TRR183 (project B02) and grants SH 81/8-1 and GO 1405/7-1, from the German Federal Ministry for Education and Research (BMBF), Project No. 13N16201 NiQ, from the National Science Foundation (NSF) – Binational Science Foundation (NSF) – Binational Science Foundation (BSF), grant 2023666, and from Berlin Quantum (BQ), an initiative endowed by the Innovation Promotion Fund of the city of Berlin, is gratefully acknowledged.

#### IV. METHODS

## Appendix A: Repeated measurements are formally equivalent to coupling to a real bath

A sequence of system-meter interactions is known to be equivalent with system interacting with a bath consisting of all meters simultaneously [69, 70]. Here we extend this to randomized meters and system-meter interactions, that is we show that, on average, repeated measurements with meter qubits that are initialized in their ground state but with random level splitting and random system-meter interactions mimic the coupling to a continuum of bath modes. We use the result of section II A: The average of the CPTP map of a system undergoing random measurements is given by the CPTP map of a single system-meter configuration, which is then averaged over all possible configurations (3). We consider the system-meter configuration to be specified by the meter splitting  $\omega_{\rm M}$  and the system-meter interaction  $H_{\rm SM}$ .

In the first step, we derive an explicit expression for the map (3) to second order in  $\gamma$ , averaging over systemmeter configurations. Thereafter, we follow the same procedure to find an expression for the CPTP map obtained for a system coupled simultaneously to all meters that entered the average in step 1. Let the system and meter(s) be governed by

$$H_{\text{tot}} = H_{\text{S}} + H_{\text{SM}} + H_{\text{M}},\tag{A1}$$

$$H_{\rm M} = \frac{\omega_{\rm M}}{2} \, \tau_z,\tag{A2}$$

$$H_{\rm SM} = \gamma A \otimes \tau_x, \tag{A3}$$

where A is the operator that couples the system to the meter. We rewrite A in terms of eigenoperators w.r.t.  $H_{\rm S}$  as

$$A = \sum_{\omega > 0} \left[ A(\omega) + A^{\dagger}(\omega) \right], \tag{A4}$$

$$A(\omega) = \sum_{\epsilon' - \epsilon = \omega}^{\omega + \omega} \Pi(\epsilon) A \Pi(\epsilon'), \tag{A5}$$

where  $\Pi(\epsilon)$  is the projector onto eigenstates of  $H_{\rm S}$  with eigenenergy  $\epsilon$ . This notation facilitates going to the interaction picture w.r.t.  $H_{\rm S}+H_{\rm M}$ , and we obtain the interaction-picture Hamiltonian:

$$H_{\rm I}(t) = \gamma \sum_{\omega > 0} \left[ A(\omega) e^{-i(\omega - \omega_{\rm M})t} + A^{\dagger}(\omega) e^{i(\omega + \omega_{\rm M})t} \right] \tau_{+} + \text{H.c.}$$
(A6)

Now, consider the Dyson series for weak couplings. To be precise, weak coupling means  $\gamma \ll J_{\rm S} \equiv \max_{1 \leq i \leq n} |\lambda_i(H_{\rm S})|$ , i.e., one needs to compare the coupling strength to the spectral radius of the system's Hamiltonian. To first order in  $\gamma/J_{\rm S}$ , the Dyson series becomes

$$U(t) = \mathbb{I} - i \int_0^t H_{\mathcal{I}}(t') dt'. \tag{A7}$$

Using Eq. (2), we find the CPTP map:

$$\mathcal{V}(t, \omega_{\mathrm{M}}) = U_{00}(t, \omega_{\mathrm{M}}) \bullet U_{00}^{\dagger}(t, \omega_{\mathrm{M}})$$
$$+ U_{10}(t, \omega_{\mathrm{M}}) \bullet U_{10}^{\dagger}(t, \omega_{\mathrm{M}}), \tag{A8}$$

$$U_{00}(t, \omega_{\rm M}) = \mathbb{I},\tag{A9}$$

$$U_{10}(t, \omega_{\rm M}) = -i\gamma t \sum_{\omega > 0} \left[ A(\omega) e^{-\frac{i}{2}(\omega - \omega_{\rm M})t} \operatorname{sinc}\left(\frac{\omega - \omega_{\rm M}}{2}t\right) \right]$$

$$+A^{\dagger}(\omega)e^{\frac{i}{2}(\omega+\omega_{\rm M})t}\operatorname{sinc}\left(\frac{\omega+\omega_{\rm M}}{2}t\right),$$
 (A10)

where  $\operatorname{sin}(x) = \sin(x)/x$  is the unnormalized sinc function. If the meter splitting at each iteration is drawn uniformly from the interval  $[0, \omega_{\mathrm{M,max}}]$ , then the configuration-averaged CPTP map becomes

$$\bar{\mathcal{V}}(t) = \mathbb{I} + \frac{1}{\omega_{\mathrm{M,max}}} \int_0^{\omega_{\mathrm{M,max}}} U_{10}(t, \omega_{\mathrm{M}}) \bullet U_{10}(t, \omega_{\mathrm{M}}) d\omega_{\mathrm{M}}.$$
(A11)

In the second step, we consider a system coupled to all meter configurations in the above average at the same time. While the system Hamiltonian is identical to that in step 1, the meter's and interaction-picture coupling Hamiltonians now take the form

$$\check{H}_{\rm M} = \int_0^{\omega_{\rm M,max}} \tau_z \left(\omega_{\rm M}\right) d\omega_{\rm M},\tag{A12}$$

$$\check{H}_{I}(t) = \gamma \frac{1}{\omega_{\mathrm{M,max}}} \sum_{\omega > 0} \int_{0}^{\omega_{\mathrm{M,max}}} \left[ A(\omega) \, \tau_{+}(\omega_{\mathrm{M}}) \, e^{-i(\omega - \omega_{\mathrm{M}})t} \right]$$

$$+A^{\dagger}(\omega)\tau_{+}(\omega_{\rm M})e^{i(\omega+\omega_{\rm M})t}d\omega_{\rm M} + \text{H.c.}$$
 (A13)

where  $\tau\left(\omega_{\mathrm{M}}\right)$  are the operators acting on the meter with splitting  $\omega_{\mathrm{M}}$  in the "bath" of meters. Invoking again the Dyson series to first order in  $\gamma$  and using Eq. (2), we find the CPTP map to be

$$\dot{\mathcal{V}}(t) = U_{\vec{0}\vec{0}}(t) \bullet U_{\vec{0}\vec{0}}^{\dagger}(t) + \sum_{i=1}^{N_m} U_{\hat{e}_i\vec{0}}(t) \bullet U_{\hat{e}_i\vec{0}}^{\dagger}(t), \quad (A14)$$

$$U_{\vec{0}\vec{0}}(t) = \mathbb{I},\tag{A15}$$

where  $N_m$  is the number of bath modes and the sum should be appropriately replaced by an integral

$$\sum_{i=1}^{N_m} \longrightarrow \int_0^{\omega_{\mathrm{M,max}}} d\omega_{\mathrm{M}}.$$

This yields

$$\check{\mathcal{V}}(t) = \mathbb{I} + \frac{1}{\omega_{\mathrm{M,max}}} \int_0^{\omega_{\mathrm{M,max}}} d\omega_{\mathrm{M}} \, \check{U}_{10}(t, \omega_{\mathrm{M}}) \bullet \check{U}_{10}^{\dagger}(t, \omega_{\mathrm{M}})$$
(A16)

with  $U_{10}(t,\omega_{\rm M})=\check{U}_{10}(t,\omega_{\rm M})$ , i.e., we obtain the same expression as in step 1. In conclusion, the CPTP map obtained by performing an average over system-meter configurations randomly drawn at every measurement interval is formally equivalent to a system coupled simultaneously to the continuum of configurations. The latter describes coupling to a continuum of bath modes.

#### Appendix B: The steady state is the ground state

In this section, we will show that, within our cooling protocol, the steady state of the system generically becomes the ground state in the limit of long interaction times  $t_M \to \infty$ . Before presenting the proof, let us recall that, generically, the CPTP map on the system  $\mathcal{V}$ , obtained from the joint unitary evolution generated by  $H_{\rm S} + H_{\rm M} + H_{\rm SM}$  by tracing out the state of the meter, will be contracting and therefore have a steady state unless  $H_{\rm SM}$  is trivial. In order to see this, we remind ourselves that any contracting CPTP map has a steady state, or, conversely, a CPTP map has no steady state iff it is unitary and maps pure states to pure states. Now, we are interested in interactions  $H_{\rm SM}$  that are non-trivial in the sense that  $H_{\rm SM}$  acts non-trivially on both the system and the meter. In the simplest case considered in this work, we write  $H_{\rm SM} = A \otimes B$ . This implies that under the joint unitary

$$U = e^{-i(H_{\rm S} + H_{\rm M} + H_{\rm SM})t_{\rm M}}$$

there exist some pure product state  $|\psi_0\rangle_{\rm M}\otimes|\phi_0\rangle_{\rm S}$  that will be entangled through the action of U. Therefore, after tracing out the meter, the system's state is

$$\rho_{\rm S} = \operatorname{tr}_{\rm M} U |\psi_0\rangle\langle\psi_0|_{\rm M} |\phi_0\rangle\langle\phi_0|_{\rm S} U^{\dagger},$$

which is a mixed state, indicating the entanglement generated by U. We conclude that the CPTP map on S is contracting because it is not unitary and, therefore, has at least one steady state.

Let us also note that we are considering the steady state of the CPTP map  $\bar{\mathcal{V}}$ . This means that it is the state obtained after an infinite but discrete number of applications of  $\bar{\mathcal{V}}$ . As such, the state after n applications is  $\rho(n) = \bar{\mathcal{V}}^n \rho(0)$  at the corresponding time of the n-th meter reset  $t = nt_{\rm M}$ . Therefore, the steady state extracted

from  $\bar{\mathcal{V}}$  should be considered a *stroboscopic* steady state, i.e., for  $n \to \infty$  it is the state the system assumes at  $t = nt_{\rm M}$ . Even though the system may well be converged for sufficiently large n, it can still undergo fluctuations between meter resets, and one should only consider the system right after the meter has been reset and not during a period of system-meter coupling. These fluctuations between meter resets can be observed in Fig. 3a.

Now, to prove that the system's ground state is such a steady state, we consider again the Dyson series (A11) and apply it to some state  $\rho$ . For the sake of readability, we omit the average over  $\omega_{\rm M}$  for now and consider only a single coupling operator A. The average over A can be performed at the end of the calculation. The map yields:

$$\rho' = \rho$$

$$+ \sum_{\omega,\omega'>0} a_{-}(\omega, \omega_{\mathrm{M}}) a_{-}^{*}(\omega', \omega_{\mathrm{M}}) A(\omega) \rho A^{\dagger}(\omega')$$

$$+ \sum_{\omega,\omega'>0} a_{+}(\omega, \omega_{\mathrm{M}}) a_{+}^{*}(\omega', \omega_{\mathrm{M}}) A^{\dagger}(\omega) \rho A(\omega')$$

$$+ \sum_{\omega,\omega'>0} a_{-}(\omega, \omega_{\mathrm{M}}) a_{+}^{*}(\omega', \omega_{\mathrm{M}}) A(\omega) \rho A(\omega')$$

$$+ \sum_{\omega,\omega'>0} a_{+}(\omega, \omega_{\mathrm{M}}) a_{-}^{*}(\omega', \omega_{\mathrm{M}}) A^{\dagger}(\omega) \rho A^{\dagger}(\omega') ,$$

where the coefficients are given by

$$a_{\pm}(\omega, \omega_{\rm M}) = \gamma \frac{e^{\pm \frac{i}{2}(\omega \pm \omega_{\rm M})t}}{\omega \pm \omega_{\rm M}} \sin\left(\frac{\omega \pm \omega_{\rm M}}{2}t\right).$$
 (B2)

In the limit of a large measurement duration, we can replace them with

$$a_{+}(\omega, \omega_{\rm M}) = \gamma \,\omega_{\rm M}(\omega \pm \omega_{\rm M}).$$
 (B3)

Taking into account that  $\omega_{\rm M} > 0$  and that the sum above runs only over positive  $\omega, \omega'$ , find that the expression simplifies to

$$\rho' = \rho + \frac{\gamma^2}{\omega_{\mathrm{M,max}}} \int_0^{\omega_{\mathrm{M,max}}} A(\omega_{\mathrm{M}}) \rho A^{\dagger}(\omega_{\mathrm{M}}) d\omega_{\mathrm{M}}, \quad (B4)$$

where we have introduced the average over  $\omega_{\rm M}$ . Note that the Dyson series (A11) only yields a unitary operator to the corresponding order in  $\gamma$ . To correct for this, we renormalize the state:

$$\rho' \mapsto \frac{1}{\operatorname{tr} \rho'} \rho'.$$
 (B5)

We are interested in the steady state of this map. A steady state has to be an eigenstate of the second part of the expression, such that we seek

$$\frac{\gamma^{2}}{\omega_{\mathrm{M,max}}} \int_{0}^{\omega_{\mathrm{M,max}}} A(\omega_{\mathrm{M}}) \rho A^{\dagger}(\omega_{\mathrm{M}}) d\omega_{\mathrm{M}} = \lambda \rho. \quad (B6)$$

We now make a crucial assumption: For every excited eigenstate  $H_{\rm S} |\epsilon'\rangle = \epsilon' |\epsilon'\rangle$  with  $\epsilon' > 0$ , there exists some

 $\omega_{\mathrm{M}}$  such that the coupling operator A couples it to some eigenstate lower in energy, i.e.  $\langle \epsilon | A | \epsilon' \rangle \neq 0$  for all  $\epsilon' > 0$  and some  $\epsilon < \epsilon'$ . Under this assumption, the operator  $A(\omega_{\mathrm{M}})$  effects a jump between eigenstates of  $H_{\mathrm{S}}$  with transition energy  $\omega_{\mathrm{M}}$  from the energetically higher eigenspace to the lower one.

We show that once the system is in its ground-state manifold, it is trapped there. To that end, consider a state with well-defined energy  $\epsilon$  where taking  $\epsilon=0$  corresponds to the ground state:

$$\rho = \sum_{i} p_i |\epsilon_i\rangle \langle \epsilon_i|. \tag{B7}$$

We now analyze the integrand  $A(\omega_{\rm M}) \rho A^{\dagger}(\omega_{\rm M})$  above in two steps: First, we show that the  $\omega_{\rm M}=0$  contribution leaves the system energy unchanged, then we consider transitions between eigenspaces with  $\omega_{\rm M}>0$ . In both cases, we need to compute

$$A(\omega_{\rm M}) \rho A^{\dagger}(\omega_{\rm M}) = \sum_{i} p_{i} A(\omega_{\rm M}) |\epsilon_{i}\rangle\langle\epsilon_{i}| A^{\dagger}(\omega_{\rm M}). \quad (B8)$$

We focus on

$$A(\omega_{\mathrm{M}}) |\epsilon_{i}\rangle\langle\epsilon_{i}| A^{\dagger}(\omega_{\mathrm{M}})$$

$$= \sum_{\mu'-\mu=\omega_{\mathrm{M}}} \sum_{\nu'-\nu=\omega_{\mathrm{M}}} \Pi(\mu) A\Pi(\mu') |\epsilon_{i}\rangle\langle\epsilon_{i}| \Pi(\nu') A\Pi(\nu)$$

$$= \sum_{\epsilon-\mu=\omega_{\mathrm{M}}} \sum_{\epsilon-\nu=\omega_{\mathrm{M}}} \Pi(\mu) A |\epsilon_{i}\rangle\langle\epsilon_{i}| A\Pi(\nu)$$

$$= \Pi(\epsilon-\omega_{\mathrm{M}}) A |\epsilon_{i}\rangle\langle\epsilon_{i}| A\Pi(\epsilon-\omega_{\mathrm{M}}).$$
(B9)

Thus, we find

$$A(\omega_{\rm M})\rho A^{\dagger}(\omega_{\rm M}) = \sum_{i} p_{i} \Pi(\epsilon - \omega_{\rm M}) A |\epsilon_{i}\rangle\langle\epsilon_{i}| A \Pi(\epsilon - \omega_{\rm M}),$$
(B10)

and we observe that  $A\left(\omega_{\mathrm{M}}\right)\rho A^{\dagger}\left(\omega_{\mathrm{M}}\right)$  is supported only in the  $\epsilon-\omega_{\mathrm{M}}$  eigenspace. It vanishes if  $\epsilon-\omega_{\mathrm{M}}$  is not an eigenenergy of the system and in particular also when  $\epsilon-\omega_{\mathrm{M}}<0$ . For  $\omega_{\mathrm{M}}=0$ ,  $A\left(0\right)\rho A^{\dagger}\left(0\right)$  remains in its original  $\epsilon$  eigenspace, its energy expectation value does not change.

Now consider a ground state  $\epsilon=0$  and denote it with  $\rho_0=\sum_i p_{i,0}\,|0_i\rangle\langle 0_i|$ . The  $\omega_{\rm M}=0$  contribution can only change the state within the  $\epsilon=0$  eigenspace but does not change its energy. Any  $\omega_{\rm M}>0$  contribution vanishes because  $\epsilon-\omega_{\rm M}<0$ . We conclude that then

$$\rho_0' = \rho_0 + \sum_i p_{i,0} \Pi(0) A |0_i\rangle\langle 0_i| A\Pi(0).$$
 (B11)

After normalization, the system energy is computed to

$$E'_{\rm S} = \operatorname{tr}(H_{\rm S}\rho'_0) = \operatorname{tr}(H_{\rm S}\rho_0) = 0$$
 (B12)

and hence, the ground space is steady.

## Appendix C: Cooling and heating of a single qubit for the steering-type system-meter coupling

We derive an explicit form of the the system energy after the n-th iteration of the protocol for a single qubit system coupled to the meter via Eq. (10). The matrix representation of the total Hamiltonian takes the form

$$H_{\text{tot}} = \frac{1}{2} \begin{pmatrix} \omega_{\text{M}} + \omega_{\text{S}} & \gamma & \gamma \\ \omega_{\text{M}} - \omega_{\text{S}} & \gamma & \gamma \\ \gamma & -\omega_{\text{M}} + \omega_{\text{S}} & -\omega_{\text{M}} - \omega_{\text{S}} \end{pmatrix},$$
(C1)

where we assume  $\omega_{\rm M} > 0$ . We find its eigenvalues to be

$$\epsilon_{1,2} = \pm \mu \equiv \pm \sqrt{\gamma^2 + (\omega_S + \omega_M)^2},$$
 (C2)

$$\epsilon_{3,4} = \pm \nu \equiv \pm \sqrt{\gamma^2 + (\omega_{\rm S} - \omega_{\rm M})^2}$$
. (C3)

At any stage of the cooling process, after resetting the meter, the system and meter are in a product state. Ideally, the meter qubit should be prepared in its ground state. Here, we also consider imperfectly prepared meters by assuming that the meter is initialized in a thermal state with occupation number  $n_{\rm M}$ 

$$\rho_{\rm M} = \frac{e^{-(\beta_{\rm M}\omega_{\rm M}/2)\tau_z}}{\operatorname{tr} e^{-(\beta_{\rm M}\omega_{\rm M}/2)\tau_z}} = \operatorname{diag}(n_{\rm M}, 1 - n_{\rm M}), \quad (C4)$$

$$n_{\rm M} = \frac{1}{1 + e^{\beta_{\rm M}\omega_{\rm M}}} \,. \tag{C5}$$

After resetting the meter to  $\rho_{\rm M}$ , system and meter are in the product state

$$\rho(n) = \rho_{\mathcal{M}} \otimes \rho_{\mathcal{S}}(n), \tag{C6}$$

where n counts the number of past iterations of the process. The system's energy at the end of the (n+1)-th iteration is given by

$$E_{\rm S}(n+1) = \text{tr} \left[ H_{\rm S} \rho_{\rm S}(n+1) \right],$$
 (C7)

$$\rho(n+1) = e^{-iH_{\text{tot}}t_M}\rho(n) e^{iH_{\text{tot}}t_M}.$$
 (C8)

Notably, we find that  $E_{\rm S}(n+1)$  does not depend on any coherences in  $\rho_{\rm S}(n)$  but just on the system energy at the end of the n-th iteration. This allows us to write:

$$E_{\rm S}(n+1) = E_{\rm S}(n) + E_{\mu}(n) + E_{\nu}(n),$$
 (C9)

$$E_{\mu}(n) = \frac{\gamma^2}{4\mu^2} \left( \frac{\widetilde{\omega_S}}{2} - E_S(n) \right) \sin^2 \frac{\mu t}{2}, \quad (C10)$$

$$E_{\nu}(n) = -\frac{\gamma^2}{4\nu^2} \left( \frac{\widetilde{\omega_{S}}}{2} + E_{S}(n) \right) \sin^2 \frac{\nu t}{2}, \qquad (C11)$$

and we have introduced

$$\widetilde{\omega_{\rm S}} = \omega_{\rm S} \left( 1 - 2n_{\rm M} \right).$$
 (C12)

Now consider the RWA regime (11b)-(11c), which leads

$$\mu \gg \nu$$
 for  $\omega_{\rm S} > 0$ , (C13)

$$\mu \ll \nu$$
 for  $\omega_{\rm S} < 0$ . (C14)

We associate the co- and counter-rotating processes with

$$E_{\rm co} = E_{\nu}, \qquad E_{\rm counter} = E_{\mu} \qquad \text{for } \omega_{\rm S} > 0, \quad \text{(C15)}$$
  
 $E_{\rm co} = E_{\mu}, \qquad E_{\rm counter} = E_{\nu} \qquad \text{for } \omega_{\rm S} < 0, \quad \text{(C16)}$ 

$$E_{\rm co} = E_{\nu}$$
,  $E_{\rm counter} = E_{\nu}$  for  $\omega_{\rm S} < 0$ , (C16)

which can be verified by repeating the above calculation after performing the RWA. We observe that the corotating process leads to a slow oscillation in the system energy associated with energy flow towards the meter. The counter-rotating terms, on the other hand, lead to an increase in both system and meter energy due to negative energy associated with  $H_{\rm SM}$ . If the counter-rotating terms dominate, one may find that the system is heated instead of cooled. This is illustrated in Fig. 3b.

One can solve the recursion (C9) to find

$$E_{S}(n) = \frac{\mu^{2} \left( E_{S}(0) + \frac{\widetilde{\omega_{S}}}{2} \right) \sin^{2} \frac{\nu t_{M}}{2} + \nu^{2} \left( E_{S}(0) - \frac{\widetilde{\omega_{S}}}{2} \right) \sin^{2} \frac{\mu t_{M}}{2}}{\mu^{2} \sin^{2} \frac{\nu t_{M}}{2} + \nu^{2} \sin^{2} \frac{\mu t_{M}}{2}} \left( 1 - \frac{\gamma^{2}}{\mu^{2}} \sin^{2} \frac{\mu t_{M}}{2} - \frac{\gamma^{2}}{\nu^{2}} \sin^{2} \frac{\nu t_{M}}{2} \right)^{n}} - \frac{\widetilde{\omega_{S}}}{2} \frac{\mu^{2} \sin^{2} \frac{\nu t_{M}}{2} - \nu^{2} \sin^{2} \frac{\mu t_{M}}{2}}{\mu^{2} \sin^{2} \frac{\nu t_{M}}{2} + \nu^{2} \sin^{2} \frac{\mu t_{M}}{2}}{\mu^{2}}.$$
(C17)

Now, we focus on the limit  $n \to \infty$ . To that end, inspect the term  $(...)^n$ . We find that with  $\gamma^2 \leq \mu^2, \nu^2$ , its content lies in [-1,1]. Therefore, except for pathological choice of parameters of measure 0, this term vanishes as  $n \to \infty$ . The asymptotic system energy becomes

$$E_{\rm S}(n \to \infty) = -\frac{\widetilde{\omega}_{\rm S}}{2} \frac{\mu^2 \sin^2 \frac{\nu t_{\rm M}}{2} - \nu^2 \sin^2 \frac{\mu t_{\rm M}}{2}}{\mu^2 \sin^2 \frac{\nu t_{\rm M}}{2} + \nu^2 \sin^2 \frac{\mu t_{\rm M}}{2}}.$$
 (C18)

This is the energy of the system in its steady state, and we show it in Fig. 3b.

The solutions (C17) and (C18) are exact. Now, we focus again on the RWA parameter regime (11b)-(11c). To first order in the ratio  $r = \nu/\mu$  for  $\omega_{\rm S} > 0$  resp. 1/r for  $\omega_{\rm S} < 0$ , the asymptotic system energy becomes

$$E_{\rm S}(n \to \infty) = \frac{\widetilde{\omega_{\rm S}}}{2} \begin{cases} 1 - \frac{\mu^2 t_{\rm M}^2}{\mu^2 t_{\rm M}^2 + 2\sin^2\frac{\mu t_{\rm M}}{2}}, & \omega_{\rm S} > 0, \\ \frac{\left(\frac{\nu t_{\rm M}}{2}\right)^2 - \sin^2\frac{\nu t_{\rm M}}{2}}{\left(\frac{\nu t_{\rm M}}{2}\right)^2 + \sin^2\frac{\nu t_{\rm M}}{2}}, & \omega_{\rm S} < 0, \end{cases}$$
(C19)

If we choose the interval length  $t_{\rm M}\gg 1/\mu$  and  $t_{\rm M}\gg 1/\nu$  for  $\omega_{\rm S}>0$  and  $\omega_{\rm S}<0$ , respectively, the system energy becomes

$$E_{\rm S}(n \to \infty) = -\frac{|\omega_{\rm S}|}{2} (1 - 2n_{\rm M}),$$
 (C20)

which is the ground-state energy, irrespective of the sign of  $\omega_{\rm S}$  for perfectly prepared meters with  $n_{\rm M}=0$ . If the meter is prepared in a thermal state with finite inverse temperature  $\beta_{\rm M}$ , we expect the meter's occupation number to be copied over to the system. That is, the system's steady state is  $\rho_{\infty}=\rho_{\rm M}$ . The effective inverse temperature of the system associated with this state is

$$\beta_{\rm S} = \beta_{\rm M} \frac{\omega_{\rm M}}{\omega_{\rm S}}.\tag{C21}$$

# Appendix D: RWA: Perturbation theory, validity, and revival of counter-rotating terms

Here, we address the RWA in more detail and demonstrate why the validity of the RWA is determined by Eqs. (11b)-(11c) of the main text. We argue that it

can be understood as an interference phenomenon where the magnitude of fast-oscillating (non-secular or counterrotating) terms collapses when compared to the slow oscillating (secular or co-rotating) ones. Like with other interference phenomena, this implies that the counterrotating terms are "revived" at some point in time (cf. collapse and revival of the excited-state population in the Jaynes-Cummings model when the cavity is in a coherent state). The purpose of this subsection is also to take the RWA beyond the folklore of saying "fast oscillations average out". In doing so, we focus on the situation at hand: two qubits coupled with an  $\sigma_x \tau_x$  interaction via the Hamiltonian (10).

The RWA is a perturbative approximation: The interaction strength  $\gamma$  is assumed to be weak w.r.t. the bare system Hamiltonian. Its spectral radius is given by  $(\omega_S + \omega_M)/2$ . Therefore, the first condition that needs to be satisfied is  $\gamma \ll (\omega_S + \omega_M)/2$ . In this case, we can treat the qubit-qubit coupling as a perturbation. Before doing so, we transform into the interaction picture w.r.t. the bare qubit Hamiltonians. We obtain

$$H_{\rm rot}(t) = \frac{\gamma}{2} \left[ \sigma_+ \tau_+ e^{i(\omega_{\rm S} + \omega_{\rm M})t/2} + \sigma_- \tau_+ e^{-i(\omega_{\rm S} - \omega_{\rm M})t/2} \right] + \text{H.c.}.$$
(D1)

For weak coupling, the time-evolution operator can be expressed to first order in  $\gamma/\omega_{\rm S}$  as

$$U_{I}(0,t) = \mathcal{T} \exp\left\{-i \int_{0}^{t} H_{\text{rot}}(t')dt'\right\}$$
 (D2)  
=  $\mathbb{I} - i \int_{0}^{t} H_{\text{rot}}(t')dt',$  (D3)

which is evaluated to

$$U_{I}\left(0,t\right) = \mathbb{I} - i\frac{\gamma}{2} \left[ \sigma_{+}\tau_{+} \frac{2e^{\frac{i}{2}(\omega_{S} + \omega_{M})t}}{\omega_{S} + \omega_{M}} \sin\left(\frac{\omega_{S} + \omega_{M}}{2}t\right) + \sigma_{-}\tau_{+} \frac{2e^{-\frac{i}{2}(\omega_{S} - \omega_{M})t}}{\omega_{S} - \omega_{M}} \sin\left(\frac{\omega_{S} - \omega_{M}}{2}t\right) + \text{H.c.} \right]. \tag{D4}$$

Let us assume for simplicity that  $\omega_{\rm S}, \omega_{\rm M} > 0$  and that  $|\omega_{\rm S} - \omega_{\rm M}| \ll \omega_{\rm S} + \omega_{\rm M}$ . In this case, the usual RWA procedure is to simply neglect terms oscillating with  $\omega_{\rm S} + \omega_{\rm M}$  and retain those with  $\omega_{\rm S} - \omega_{\rm M}$ . We now want to take a closer look: Consider the ratio of the counter-rotating over co-rotating amplitudes

$$r = \left| \frac{\omega_{\rm S} - \omega_{\rm M}}{\omega_{\rm S} + \omega_{\rm M}} \frac{\operatorname{sinc}\left(\frac{\omega_{\rm S} + \omega_{\rm M}}{2}t\right)}{\operatorname{sinc}\left(\frac{\omega_{\rm S} - \omega_{\rm M}}{2}t\right)} \right|. \tag{D5}$$

If  $r \ll 1$ , then the RWA is justified. In the regime where  $|\omega_S - \omega_M| \ll \omega_S + \omega_M$ , we can expand r to leading order

in  $\omega_{\rm S} - \omega_{\rm M}/(\omega_{\rm S} + \omega_{\rm M})$  to find

$$r = \left| \frac{\omega_{\rm S} - \omega_{\rm M}}{\omega_{\rm S} + \omega_{\rm M}} \operatorname{sinc} \left( \frac{\omega_{\rm S} + \omega_{\rm M}}{2} t \right) \right| + \mathcal{O}(r). \tag{D6}$$

As the magnitude of the function  $\operatorname{sinc}(x)$  decays as 1/x for large x, we conclude that the RWA is then valid for times  $t \gg 2/(\omega_{\rm S} + \omega_{\rm M})$ . There is, however, a caveat: Although  $\omega_{\rm S} - \omega_{\rm M}$  may be negligible when compared to  $\omega_{\rm S} + \omega_{\rm M}$ , as long as it is finite, it can play a role at large t. Indeed the denominator in Eq. (D5) has roots at  $t = 4\pi n/(\omega_{\rm S} - \omega_{\rm M})$  with  $n \in \mathbb{N}$ . Let's take a step back and consider how the ratio of co- and counter-rotating terms evolves: At t = 0 we have = 1. Then in the interval where

 $t \gg 2/(\omega_{\rm S} + \omega_{\rm M})$  and  $t \ll 4\pi/(\omega_{\rm S} - \omega_{\rm M})$  the co-rotating terms dominate. We interpret this as a "collapse" of counter-rotating contributions. As soon as we hit  $t = 4\pi n/(\omega_{\rm S} - \omega_{\rm M})$ , the counter-rotating terms are "revived" briefly before collapsing again. This process is depicted

in Fig. 3b. Note that although the counter-rotating terms show a revival at certain times, their magnitude relative to the co-rotating terms is suppressed by  $(\omega_S - \omega_M)/(\omega_S + \omega_M)$ .

- C. N. Cohen-Tannoudji, Manipulating atoms with photons, Rev. Mod. Phys. 70 (1998).
- [2] W. D. Phillips, Laser cooling and trapping of neutral atoms, Rev. Mod. Phys. 70 (1998).
- [3] S. Chu, The manipulation of neutral particles, Rev. Mod. Phys. 70 (1998).
- [4] D. J. Wineland, Nobel Lecture: Superposition, entanglement, and raising Schrödinger's cat, Rev. Mod. Phys. 85, 1103 (2013).
- [5] S. M. Girvin, Circuit QED: Superconducting qubits coupled to microwave photons, in *Quantum Machines: Measurement and Control of Engineered Quantum Systems*, edited by M. Devoret, B. Huard, R. Schoelkopf, and L. F. Cugliandolo (Oxford University PressOxford, 2014) 1st ed., pp. 113–256.
- [6] D. P. DiVincenzo, The Physical Implementation of Quantum Computation, Fortschr. Phys. 48, 771 (2000).
- [7] J. Preskill, Quantum Computing in the NISQ era and beyond, Quantum 2, 79 (2018), arXiv:1801.00862 [quantph].
- [8] K. Bharti, A. Cervera-Lierta, T. H. Kyaw, T. Haug, S. Alperin-Lea, A. Anand, M. Degroote, H. Heimonen, J. S. Kottmann, T. Menke, W.-K. Mok, S. Sim, L.-C. Kwek, and A. Aspuru-Guzik, Noisy intermediate-scale quantum algorithms, Rev. Mod. Phys. 94, 015004 (2022).
- [9] M. Cerezo, A. Arrasmith, R. Babbush, S. C. Benjamin, S. Endo, K. Fujii, J. R. McClean, K. Mitarai, X. Yuan, L. Cincio, and P. J. Coles, Variational quantum algorithms, Nat Rev Phys 3, 625 (2021).
- [10] D. Wecker, M. B. Hastings, and M. Troyer, Progress towards practical quantum variational algorithms, Phys. Rev. A 92, 042303 (2015).
- [11] Y. Alexeev, M. Amsler, M. A. Barroca, S. Bassini, T. Battelle, D. Camps, D. Casanova, Y. J. Choi, F. T. Chong, C. Chung, C. Codella, A. D. Córcoles, J. Cruise, A. Di Meglio, I. Duran, T. Eckl, S. Economou, S. Eidenbenz, B. Elmegreen, C. Fare, I. Faro, C. S. Fernández, R. N. B. Ferreira, K. Fuji, B. Fuller, L. Gagliardi, G. Galli, J. R. Glick, I. Gobbi, P. Gokhale, S. De La Puente Gonzalez, J. Greiner, B. Gropp, M. Grossi, E. Gull, B. Healy, M. R. Hermes, B. Huang, T. S. Humble, N. Ito, A. F. Izmaylov, A. Javadi-Abhari, D. Jennewein, S. Jha, L. Jiang, B. Jones, W. A. De Jong, P. Jurcevic, W. Kirby, S. Kister, M. Kitagawa, J. Klassen, K. Klymko, K. Koh, M. Kondo, D. M. Kürkçüoğlu, K. Kurowski, T. Laino, R. Landfield, M. Leininger, V. Leyton-Ortega, A. Li, M. Lin, J. Liu, N. Lorente, A. Luckow, S. Martiel, F. Martin-Fernandez, M. Martonosi, C. Marvinney, A. C. Medina, D. Merten, A. Mezzacapo, K. Michielsen, A. Mitra, T. Mittal, K. Moon, J. Moore, S. Mostame, M. Motta, Y.-H. Na, Y. Nam, P. Narang, Y.-y. Ohnishi, D. Ottaviani, M. Otten, S. Pakin, V. R. Pascuzzi, E. Pednault, T. Piontek, J. Pitera, P. Rall, G. S. Ravi, N. Robert-

- son, M. A. Rossi, P. Rydlichowski, H. Ryu, G. Samsonidze, M. Sato, N. Saurabh, V. Sharma, K. Sharma, S. Shin, G. Slessman, M. Steiner, I. Sitdikov, I.-S. Suh, E. D. Switzer, W. Tang, J. Thompson, S. Todo, M. C. Tran, D. Trenev, C. Trott, H.-H. Tseng, N. M. Tubman, E. Tureci, D. G. Valiñas, S. Vallecorsa, C. Wever, K. Wojciechowski, X. Wu, S. Yoo, N. Yoshioka, V. W.-z. Yu, S. Yunoki, S. Zhuk, and D. Zubarev, Quantum-centric supercomputing for materials science: A perspective on challenges and future directions, Future Generation Computer Systems 160, 666 (2024).
- [12] R. Alicki and R. Kosloff, Introduction to Quantum Thermodynamics: History and Prospects, in *Thermodynamics in the Quantum Regime*, Vol. 195, edited by F. Binder, L. A. Correa, C. Gogolin, J. Anders, and G. Adesso (Springer International Publishing, Cham, 2018) pp. 1–33.
- [13] F. Ticozzi and L. Viola, Quantum resources for purification and cooling: Fundamental limits and opportunities, Sci Rep 4, 5192 (2014).
- [14] D. Basilewitsch, J. Fischer, D. M. Reich, D. Sugny, and C. P. Koch, Fundamental bounds on qubit reset, Phys. Rev. Research 3, 013110 (2021).
- [15] N. Fitch and M. Tarbutt, Chapter three laser-cooled molecules (Academic Press, 2021) pp. 157–262.
- [16] S. Diehl, A. Micheli, A. Kantian, B. Kraus, H.-P. Büchler, and P. Zoller, Quantum states and phases in driven open quantum systems with cold atoms, Nature Phys. 4, 878 (2008).
- [17] S. Diehl, E. Rico, M. A. Baranov, and P. Zoller, Topology by dissipation in atomic quantum wires, Nature Phys 7, 971 (2011).
- [18] F. Verstraete, M. M. Wolf, and J. Ignacio Cirac, Quantum computation and quantum-state engineering driven by dissipation, Nature Phys 5, 633 (2009).
- [19] Y. Zhan, Z. Ding, J. Huhn, J. Gray, J. Preskill, G. K.-L. Chan, and L. Lin, Rapid quantum ground state preparation via dissipative dynamics (2025), arXiv:2503.15827 [quant-ph].
- [20] L. Lin, Dissipative Preparation of Many-Body Quantum States: Towards Practical Quantum Advantage (2025), arXiv:2505.21308 [quant-ph].
- [21] G. Morigi, J. Eschner, C. Cormick, Y. Lin, D. Leibfried, and D. J. Wineland, Dissipative Quantum Control of a Spin Chain, Phys. Rev. Lett. 115, 200502 (2015).
- [22] S. Roy, J. T. Chalker, I. V. Gornyi, and Y. Gefen, Measurement-induced steering of quantum systems, Phys. Rev. Research 2, 033347 (2020).
- [23] P. Kumar, K. Snizhko, and Y. Gefen, Engineering twoqubit mixed states with weak measurements, Phys. Rev. Res. 2, 042014 (2020).
- [24] Y. Herasymenko, I. Gornyi, and Y. Gefen, Measurement-Driven Navigation in Many-Body Hilbert Space: Active-Decision Steering, PRX Quantum 4, 020347 (2023).

- [25] D. Volya and P. Mishra, State Preparation on Quantum Computers via Quantum Steering, IEEE Trans. Quantum Eng. 5, 1 (2024).
- [26] S. Morales, Y. Gefen, I. Gornyi, A. Zazunov, and R. Egger, Engineering unsteerable quantum states with active feedback, Phys. Rev. Research 6, 013244 (2024).
- [27] We refer to the auxiliary qubits as the *measurement* or *meter* qubits since discarding them after their interaction with the system is equivalent to performing a projective measurement without keeping track of the outcome [81] (so-called "blind measurement" [22]).
- [28] L. Zhao, C. A. Perez-Delgado, S. C. Benjamin, and J. F. Fitzsimons, A measurement driven analog of adiabatic quantum computation for frustration-free Hamiltonians, Phys. Rev. A 100, 032331 (2019), arXiv:1706.02559 [quant-ph].
- [29] C. Noel, P. Niroula, D. Zhu, A. Risinger, L. Egan, D. Biswas, M. Cetina, A. V. Gorshkov, M. J. Gullans, D. A. Huse, and C. Monroe, Measurement-induced quantum phases realized in a trapped-ion quantum computer, Nat. Phys. 18, 760 (2022).
- [30] R. Menu, J. Langbehn, C. P. Koch, and G. Morigi, Reservoir-engineering shortcuts to adiabaticity, Phys. Rev. Research 4, 033005 (2022).
- [31] P. M. Harrington, E. J. Mueller, and K. W. Murch, Engineered Dissipation for Quantum Information Science, Nature Rev. Phys. 4, 660 (2022).
- [32] J. M. Koh, S.-N. Sun, M. Motta, and A. J. Minnich, Measurement-induced entanglement phase transition on a superconducting quantum processor with mid-circuit readout, Nat. Phys. 19, 1314 (2023).
- [33] Google Quantum AI and Collaborators, J. C. Hoke, M. Ippoliti, E. Rosenberg, D. Abanin, R. Acharya, T. I. Andersen, M. Ansmann, F. Arute, K. Arya, A. Asfaw, J. Atalava, J. C. Bardin, A. Bengtsson, G. Bortoli, A. Bourassa, J. Bovaird, L. Brill, M. Broughton, B. B. Buckley, D. A. Buell, T. Burger, B. Burkett, N. Bushnell, Z. Chen, B. Chiaro, D. Chik, J. Cogan, R. Collins, P. Conner, W. Courtney, A. L. Crook, B. Curtin, A. G. Dau, D. M. Debroy, A. Del Toro Barba, S. Demura, A. Di Paolo, I. K. Drozdov, A. Dunsworth, D. Eppens, C. Erickson, E. Farhi, R. Fatemi, V. S. Ferreira, L. F. Burgos, E. Forati, A. G. Fowler, B. Foxen, W. Giang, C. Gidney, D. Gilboa, M. Giustina, R. Gosula, J. A. Gross, S. Habegger, M. C. Hamilton, M. Hansen, M. P. Harrigan, S. D. Harrington, P. Heu, M. R. Hoffmann, S. Hong, T. Huang, A. Huff, W. J. Huggins, S. V. Isakov, J. Iveland, E. Jeffrey, Z. Jiang, C. Jones, P. Juhas, D. Kafri, K. Kechedzhi, T. Khattar, M. Khezri, M. Kieferová, S. Kim, A. Kitaev, P. V. Klimov, A. R. Klots, A. N. Korotkov, F. Kostritsa, J. M. Kreikebaum, D. Landhuis, P. Laptev, K.-M. Lau, L. Laws, J. Lee, K. W. Lee, Y. D. Lensky, B. J. Lester, A. T. Lill, W. Liu, A. Locharla, O. Martin, J. R. McClean, M. McEwen, K. C. Miao, A. Mieszala, S. Montazeri, A. Morvan, R. Movassagh, W. Mruczkiewicz, M. Neeley, C. Neill, A. Nersisyan, M. Newman, J. H. Ng, A. Nguyen, M. Nguyen, M. Y. Niu, T. E. O'Brien, S. Omonije, A. Opremcak, A. Petukhov, R. Potter, L. P. Pryadko, C. Quintana, C. Rocque, N. C. Rubin, N. Saei, D. Sank, K. Sankaragomathi, K. J. Satzinger, H. F. Schurkus, C. Schuster, M. J. Shearn, A. Shorter, N. Shutty, V. Shvarts, J. Skruzny, W. C. Smith, R. Somma, G. Sterling, D. Strain, M. Szalay, A. Torres, G. Vidal, B. Vil-

- lalonga, C. V. Heidweiller, T. White, B. W. K. Woo, C. Xing, Z. J. Yao, P. Yeh, J. Yoo, G. Young, A. Zalcman, Y. Zhang, N. Zhu, N. Zobrist, H. Neven, R. Babbush, D. Bacon, S. Boixo, J. Hilton, E. Lucero, A. Megrant, J. Kelly, Y. Chen, V. Smelyanskiy, X. Mi, V. Khemani, and P. Roushan, Measurement-induced entanglement and teleportation on a noisy quantum processor, Nature 622, 481 (2023).
- [34] T. S. Cubitt, Dissipative ground state preparation and the Dissipative Quantum Eigensolver (2023), arXiv:2303.11962 [quant-ph].
- [35] K. C. Smith, E. Crane, N. Wiebe, and S. Girvin, Deterministic Constant-Depth Preparation of the AKLT State on a Quantum Processor Using Fusion Measurements, PRX Quantum 4, 020315 (2023).
- [36] A. Sriram, T. Rakovszky, V. Khemani, and M. Ippoliti, Topology, criticality, and dynamically generated qubits in a stochastic measurement-only Kitaev model, Phys. Rev. B 108, 094304 (2023).
- [37] A. Lavasani, Z.-X. Luo, and S. Vijay, Monitored quantum dynamics and the Kitaev spin liquid, Phys. Rev. B 108, 115135 (2023).
- [38] A. Matthies, M. Rudner, A. Rosch, and E. Berg, Programmable adiabatic demagnetization for systems with trivial and topological excitations, Quantum 8, 1505 (2024), arXiv:2210.17256 [quant-ph].
- [39] D. A. Puente, F. Motzoi, T. Calarco, G. Morigi, and M. Rizzi, Quantum state preparation via engineered ancilla resetting, Quantum 8, 1299 (2024), arXiv:2305.08641 [quant-ph].
- [40] T. Chen and T. Byrnes, Efficient preparation of the AKLT State with Measurement-based Imaginary Time Evolution, Quantum 8, 1557 (2024), arXiv:2310.06031 [quant-ph].
- [41] B. M. Terhal and D. P. DiVincenzo, Problem of equilibration and the computation of correlation functions on a quantum computer, Phys. Rev. A 61, 022301 (2000).
- [42] S. Pielawa, G. Morigi, D. Vitali, and L. Davidovich, Generation of Einstein-Podolsky-Rosen-Entangled Radiation through an Atomic Reservoir, Phys. Rev. Lett. 98, 240401 (2007).
- [43] B. Kraus, H. P. Büchler, S. Diehl, A. Kantian, A. Micheli, and P. Zoller, Preparation of entangled states by quantum Markov processes, Phys. Rev. A 78, 042307 (2008).
- [44] K. Rojan, D. M. Reich, I. Dotsenko, J.-M. Raimond, C. P. Koch, and G. Morigi, Arbitrary-quantum-state preparation of a harmonic oscillator via optimal control, Phys. Rev. A 90, 023824 (2014).
- [45] T. Brown, E. Doucet, D. Ristè, G. Ribeill, K. Cicak, J. Aumentado, R. Simmonds, L. Govia, A. Kamal, and L. Ranzani, Trade off-free entanglement stabilization in a superconducting qutrit-qubit system, Nat Commun 13, 3994 (2022).
- [46] M. Metcalf, E. Stone, K. Klymko, A. F. Kemper, M. Sarovar, and W. A. De Jong, Quantum Markov chain Monte Carlo with digital dissipative dynamics on quantum computers, Quantum Sci. Technol. 7, 025017 (2022).
- [47] J. M. Kitzman, J. R. Lane, C. Undershute, P. M. Harrington, N. R. Beysengulov, C. A. Mikolas, K. W. Murch, and J. Pollanen, Phononic bath engineering of a superconducting qubit, Nat Commun 14, 3910 (2023).
- [48] J. Langbehn, K. Snizhko, I. Gornyi, G. Morigi, Y. Gefen, and C. P. Koch, Dilute Measurement-Induced Cooling into Many-Body Ground States, PRX Quantum 5,

- 030301 (2024).
- [49] X. Mi, A. A. Michailidis, S. Shabani, K. C. Miao, P. V. Klimov, J. Lloyd, E. Rosenberg, R. Acharya, I. Aleiner, T. I. Andersen, M. Ansmann, F. Arute, K. Arya, A. Asfaw, J. Atalaya, J. C. Bardin, A. Bengtsson, G. Bortoli, A. Bourassa, J. Bovaird, L. Brill, M. Broughton, B. B. Buckley, D. A. Buell, T. Burger, B. Burkett, N. Bushnell, Z. Chen, B. Chiaro, D. Chik, C. Chou, J. Cogan, R. Collins, P. Conner, W. Courtney, A. L. Crook, B. Curtin, A. G. Dau, D. M. Debroy, A. Del Toro Barba, S. Demura, A. Di Paolo, I. K. Drozdov, A. Dunsworth, C. Erickson, L. Faoro, E. Farhi, R. Fatemi, V. S. Ferreira, L. F. Burgos, E. Forati, A. G. Fowler, B. Foxen, É. Genois, W. Giang, C. Gidney, D. Gilboa, M. Giustina, R. Gosula, J. A. Gross, S. Habegger, M. C. Hamilton, M. Hansen, M. P. Harrigan, S. D. Harrington, P. Heu, M. R. Hoffmann, S. Hong, T. Huang, A. Huff, W. J. Huggins, L. B. Ioffe, S. V. Isakov, J. Iveland, E. Jeffrey, Z. Jiang, C. Jones, P. Juhas, D. Kafri, K. Kechedzhi, T. Khattar, M. Khezri, M. Kieferová, S. Kim, A. Kitaev, A. R. Klots, A. N. Korotkov, F. Kostritsa, J. M. Kreikebaum, D. Landhuis, P. Laptev, K.-M. Lau, L. Laws, J. Lee, K. W. Lee, Y. D. Lensky, B. J. Lester, A. T. Lill, W. Liu, A. Locharla, F. D. Malone, O. Martin, J. R. McClean, M. McEwen, A. Mieszala, S. Montazeri, A. Morvan, R. Movassagh, W. Mruczkiewicz, M. Neeley, C. Neill, A. Nersisyan, M. Newman, J. H. Ng, A. Nguyen, M. Nguyen, M. Y. Niu, T. E. O'Brien, A. Opremcak, A. Petukhov, R. Potter, L. P. Pryadko, C. Quintana, C. Rocque, N. C. Rubin, N. Saei, D. Sank, K. Sankaragomathi, K. J. Satzinger, H. F. Schurkus, C. Schuster, M. J. Shearn, A. Shorter, N. Shutty, V. Shvarts, J. Skruzny, W. C. Smith, R. Somma, G. Sterling, D. Strain, M. Szalav. A. Torres, G. Vidal, B. Villalonga, C. V. Heidweiller, T. White, B. W. K. Woo, C. Xing, Z. J. Yao, P. Yeh, J. Yoo, G. Young, A. Zalcman, Y. Zhang, N. Zhu, N. Zobrist, H. Neven, R. Babbush, D. Bacon, S. Boixo, J. Hilton, E. Lucero, A. Megrant, J. Kelly, Y. Chen, P. Roushan, V. Smelyanskiy, and D. A. Abanin, Stable quantum-correlated many-body states through engineered dissipation, Science 383, 1332 (2024).
- [50] Z. Ding, C.-F. Chen, and L. Lin, Single-ancilla ground state preparation via Lindbladians, Phys. Rev. Research 6, 033147 (2024).
- [51] J. Lloyd, A. A. Michailidis, X. Mi, V. Smelyanskiy, and D. A. Abanin, Quasiparticle Cooling Algorithms for Quantum Many-Body State Preparation, PRX Quantum 6, 010361 (2025).
- [52] G. Kishony, M. S. Rudner, A. Rosch, and E. Berg, Gauged Cooling of Topological Excitations and Emergent Fermions on Quantum Simulators, Phys. Rev. Lett. 134, 086503 (2025).
- [53] P. O. Boykin, T. Mor, V. Roychowdhury, F. Vatan, and R. Vrijen, Algorithmic cooling and scalable NMR quantum computers, Proc. Natl. Acad. Sci. U.S.A. 99, 3388 (2002).
- [54] J. M. Fernandez, S. Lloyd, T. Mor, and V. Roychowdhury, ALGORITHMIC COOLING OF SPINS: A PRAC-TICABLE METHOD FOR INCREASING POLARIZA-TION, Int. J. Quantum Inform. 02, 461 (2004).
- [55] L. J. Schulman, T. Mor, and Y. Weinstein, Physical Limits of Heat-Bath Algorithmic Cooling, SIAM J. Comput. 36, 1729 (2007).
- [56] N. Linden, S. Popescu, and P. Skrzypczyk, How Small

- Can Thermal Machines Be? The Smallest Possible Refrigerator, Phys. Rev. Lett. **105**, 130401 (2010).
- [57] D. K. Park, N. A. Rodriguez-Briones, G. Feng, R. Rahimi, J. Baugh, and R. Laflamme, Heat Bath Algorithmic Cooling with Spins: Review and Prospects, in *Electron Spin Resonance (ESR) Based Quantum Computing*, Vol. 31, edited by T. Takui, L. Berliner, and G. Hanson (Springer New York, New York, NY, 2016) pp. 227–255.
- [58] T. Fogarty, H. Landa, C. Cormick, and G. Morigi, Optomechanical many-body cooling to the ground state using frustration, Phys. Rev. A 94, 023844 (2016).
- [59] M. Metcalf, J. E. Moussa, W. A. De Jong, and M. Sarovar, Engineered thermalization and cooling of quantum many-body systems, Phys. Rev. Research 2, 023214 (2020).
- [60] M. P. Zaletel, A. Kaufman, D. M. Stamper-Kurn, and N. Y. Yao, Preparation of Low Entropy Correlated Many-Body States via Conformal Cooling Quenches, Phys. Rev. Lett. 126, 103401 (2021).
- [61] S. Polla, Y. Herasymenko, and T. E. O'Brien, Quantum digital cooling, Phys. Rev. A 104, 012414 (2021).
- [62] J.-J. Feng, B. Wu, and F. Wilczek, Quantum Computing by Coherent Cooling, Phys. Rev. A 105, 052601 (2022).
- [63] V. Maurya, H. Zhang, D. Kowsari, A. Kuo, D. M. Hartsell, C. Miyamoto, J. Liu, S. Shanto, E. Vlachos, A. Zarassi, K. W. Murch, and E. M. Levenson-Falk, On-Demand Driven Dissipation for Cavity Reset and Cooling, PRX Quantum 5, 020321 (2024).
- [64] J. Uppalapati, P. A. McClarty, M. Haque, and S. Dutta, Anti-thermalization: Heating by cooling and vice versa (2024), arXiv:2412.07630 [cond-mat].
- [65] L. Marti, R. Mansuroglu, and M. J. Hartmann, Efficient Quantum Cooling Algorithm for Fermionic Systems, Quantum 9, 1635 (2025), arXiv:2403.14506 [quant-ph].
- [66] D. Molpeceres, S. Lu, J. I. Cirac, and B. Kraus, Quantum algorithms for cooling: A simple case study (2025), arXiv:2503.24330 [quant-ph].
- [67] V. Scarani, M. Ziman, P. Štelmachovič, N. Gisin, and V. Bužek, Thermalizing Quantum Machines: Dissipation and Entanglement, Phys. Rev. Lett. 88, 097905 (2002).
- [68] F. Ciccarello, Collision models in quantum optics, Quantum Measurements and Quantum Metrology 4, 10.1515/qmetro-2017-0007 (2017).
- [69] M. Cattaneo, G. De Chiara, S. Maniscalco, R. Zambrini, and G. L. Giorgi, Collision Models Can Efficiently Simulate Any Multipartite Markovian Quantum Dynamics, Phys. Rev. Lett. 126, 130403 (2021).
- [70] F. Ciccarello, S. Lorenzo, V. Giovannetti, and G. M. Palma, Quantum collision models: Open system dynamics from repeated interactions, Physics Reports 954, 1 (2022).
- [71] L. Magrini, P. Rosenzweig, C. Bach, A. Deutschmann-Olek, S. G. Hofer, S. Hong, N. Kiesel, A. Kugi, and M. Aspelmeyer, Real-time optimal quantum control of mechanical motion at room temperature, Nature 595, 373 (2021).
- [72] M. Kamba, R. Shimizu, and K. Aikawa, Optical cold damping of neutral nanoparticles near the ground state in an optical lattice, Opt. Express 30, 26716 (2022).
- [73] F. Tebbenjohanns, M. L. Mattana, M. Rossi, M. Frimmer, and L. Novotny, Quantum control of a nanoparticle optically levitated in cryogenic free space, Nature 595,

- 378 (2021).
- [74] S. Sugiura and M. Ueda, Quantum feedback cooling of a trapped nanoparticle by using a low-pass filter (2025), arXiv:2505.10157 [quant-ph].
- [75] A. C. Doherty and K. Jacobs, Feedback control of quantum systems using continuous state estimation, Phys. Rev. A 60, 2700 (1999).
- [76] M. Ziman, P. Štelmachovič, V. Bužek, M. Hillery, V. Scarani, and N. Gisin, Diluting quantum information: An analysis of information transfer in system-reservoir interactions, Phys. Rev. A 65, 042105 (2002).
- [77] F. Ticozzi and L. Viola, Stabilizing Entangled States with Quasi-Local Quantum Dynamical Semigroups, Phil. Trans. R. Soc. A. 370, 5259 (2012), arXiv:1112.4860 [quant-ph].
- [78] Y.-X. Wang and Y. Gefen, State Engineering of Unsteer-

- able Hamiltonians (2025), arXiv:2505.18393 [quant-ph].
- [79] C. Ramon-Escandell, A. Prositto, and D. Segal, Thermal state preparation by repeated interactions at and beyond the Lindblad limit (2025), arXiv:2506.12166 [quant-ph].
- [80] S. Morales, S. Pappalardi, and R. Egger, Towards scalable active steering protocols for genuinely entangled state manifolds, Phys. Rev. Research 7, 023170 (2025).
- [81] B.-G. Englert and G. Morigi, Five Lectures on Dissipative Master Equations, in *Coherent Evolution in Noisy Environments*, Vol. 611, edited by R. Beig, B. G. Englert, U. Frisch, P. Hänggi, K. Hepp, W. Hillebrandt, D. Imboden, R. L. Jaffe, R. Lipowsky, H. V Löhneysen, I. Ojima, D. Sornette, S. Theisen, W. Weise, J. Wess, J. Zittartz, A. Buchleitner, and K. Hornberger (Springer Berlin Heidelberg, Berlin, Heidelberg, 2002) pp. 55–106.